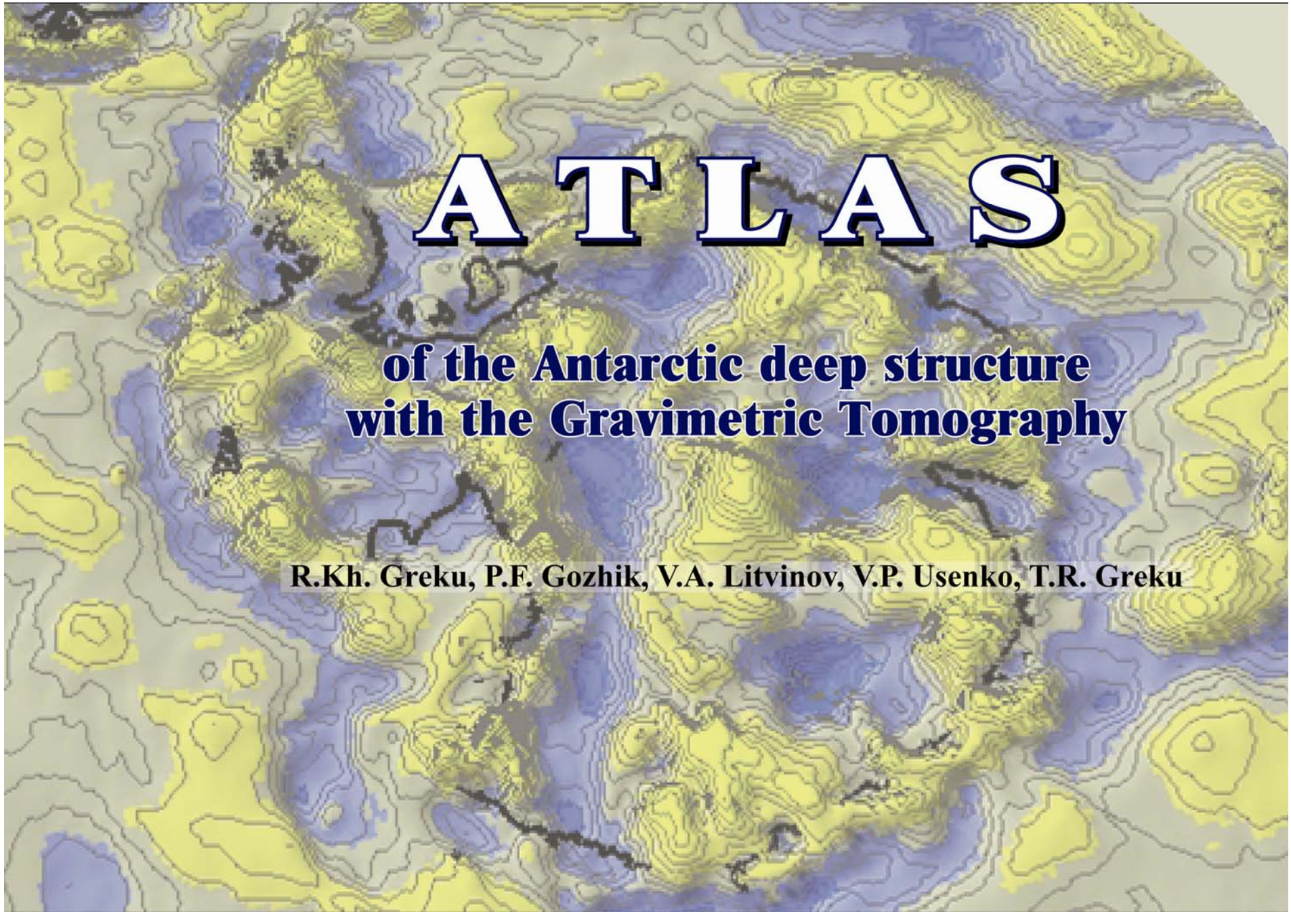

ATLAS

of the Antarctic deep structure with the Gravimetric Tomography

R.Kh. Greku, P.F. Gozhik, V.A. Litvinov, V.P. Usenko, T.R. Greku

NATIONAL ACADEMY OF SCIENCES OF UKRAINE
INSTITUTE OF GEOLOGICAL SCIENCES
NATIONAL ANTARCTIC SCIENTIFIC CENTER OF UKRAINE

Atlas of the Antarctic deep structure with the Gravimetric Tomography

R.Kh. Greku, P.F. Gozhik, V.A. Litvinov, V.P. Usenko, T. R. Greku

Kiev Ukraine
2009

Atlas of the Antarctic deep structure with the Gravimetric Tomography / Greku R.Kh., Gozhik P.F., Litvinov V.A., Usenko V.P., Greku T. R.; - Kiev, 2009.-67 pp.- ISBN 978-966-02-4937-0

The Atlas contains results of a deep structure modeling of the Antarctic and the South Ocean regions. Initial data are spherical harmonics of the EGM96 global geoid model. Dense heterogeneities are calculated using the gravimetric tomography technology. 3D images of vertical and lateral sections on different depths are presented.

Proceeding computing design: "Geographika"

ISBN 978-966-02-4937-0

Atlas of the Antarctic deep structure with the Gravimetric Tomography

CONTENTS

Introduction

The Atlas contains information on anomalous dense heterogeneities computed with the gravimetric tomography method using the EGM96 global geopotential model of the geoid. 3D images of vertical cross-sections and maps of lateral slices on different depths of the Antarctic lithosphere plate within 30°S are presented. Tectonic structure, intraplate and interplate processes of the Antarctic region are shown on the world maps and at the sections along the Antarctic Plate's boundary on spreading mid-ocean ridges at a distance more than 40,000km. The primary link of the mantle plume located in the Ross Sea area with the North America thinning structure is noted at the depth of 5300km. New information about penetrating of the Ross plume thinning hot masses into the colder crust and the lithosphere in the Australian-Antarctic Discordance and the Nazca Ridge areas was obtained from several vertical sections. Rift channels for rise of thinning material in the West Antarctic Rift System along the meridians 90°W and 170°W are shown. The channels of deep matter from the Weddell subduction zone up to the Bransfield rift system are discovered. Regional features of the Scotia Sea's deep structure and the Pacific and Atlantic mantle flows are shown along 58°S.

Atlas includes 61 maps and vertical cross-sections, some explanations and interpretation of images. The following topics are in the atlas:

I Gravimetric Tomography method and initial data;
II Interaction of Antarctica with other regions;
III Transformation of the Earth's structure in different depths within the Antarctic lithosphere plate;
IV Antarctic lithosphere boundary;
V Trans Antarctic vertical sections;
VI Sections crossing the West Antarctic
VII Detailed structural maps of the West Antarctic
VIII Regional structural features of the Scotia Plate
REFERENCES

The Atlas is prepared during the International Polar Year 2007-2009 within the framework of the POLENET Project.

I Gravimetric Tomography method and initial data

I.1 *Gravimetric Tomography*

I.1 *Gravimetric Tomography:*

1) depth of a disturbing layer

The fundamental spherical harmonical expansion of the 1/r equation for a case of internal mas potential within a sphere is used in our method for assessment of a disturbing layer's depth.

$$\frac{1}{r} = \sum_{n=o}^{\infty} \frac{\rho^n}{R^{n+1}} P_n(\cos\psi),$$

where r=distance from the sphere surface down to the disturbing mass; Ψ=angle between R and ρ.

The calculation of this formula was carried out under certain conditions, namely, n_{min}=2, Ψ=0 and then P_n (cosΨ)=1 for all of n and r=R- ρ. Thus, an appropriate n was selected by the assigned values of r, ρ and R.

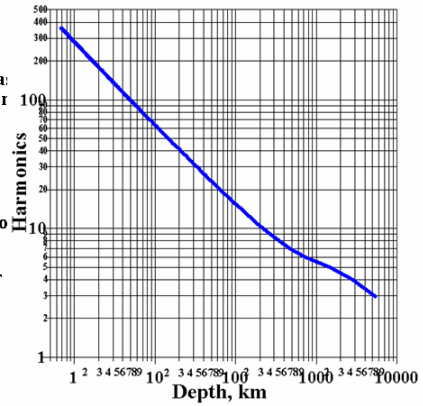

Relationship between harmonic degrees *n* and depths r of the disturbing layers of the Earth. Value n is the sum of harmonicas in a range from degree 2 up to n.

2) Determination of the harmonic density of anomalous disturbing mass.
Moritz's algorithm, 1990

$$\rho_h = \sum_{n=2}^{z}\sum_{m=0}^{n} \frac{M(2n+1)(2n+3)}{4\pi R^{n+3}} \cdot r^n (c_{mn}\cos m\lambda + s_{mn}\sin m\lambda) P_{mn}(\cos B),$$

where ρ_h=harmonic density; M=Eatrh's mass; R=Earth's radius; r^n=radius of sphere which disturbs the geopotential; P=Legendre polynomial.

I.1 *Gravimetric Tomography*

Geotectonic researches are constrained by the shortage of the deep Earth's interior data in most cases. This problem relates especially to such key remote and inaccessible areas as the Antarctic and Arctic. A known informative source of such data is the seismic tomography technology [1] in which signals of earthquakes and explosions are used. Our gravimetric tomography technique [2] is based on realization of theoretical approach by Prof. H. Moritz [3] that the Earth's equipotential surfaces coincide with surfaces of the constant density and on usage of his algorithm of determination of the harmonic dense anomalies through the spherical harmonics of the gravity potential.

Moreover, we used a well-known extracting procedure of certain harmonics (Brown 1993, Gahagan 1988) for determination of a residual (differential) geoid and for Mapping of structures in different layers, which disturb the geopotential.

Experienced geophysicists have made approximate evaluations of disturbing layers depths using the geoid harmonics. So, it was noted in the work [4] that the density inhomogeneities at the center of the Earth are responsible for harmonics of about 2≤ n ≤5, the lower mantle is responsible for the range of 2 ≤ n ≤20, and the upper mantle for the range of 2≤ n ≤100. It is supposed in another reference work [5], that harmonics of up to 8 degrees are probably caused by the impact of masses located in depths of more than 1000 km, and from 8 to 22 in depths of 50-300 km.

These assessments of a logical conformity between number of a harmonics and depth of a disturbing layer motivated us to determine a numeric dependence in this relationship.

Thus, the gravimetric tomography method includes a solution of the following tasks:

1. Determination of harmonic density of anomalous disturbing masses by the geoid spherical functions.
2. Determination of a relationship between degrees of the harmonic series expansion of the geoid topography and depths of disturbing layers of the Earth.
3. Creation and displaying of the structured model of dense inhomogeneities for the studied region.

The algorithm for calculation of anomalous harmonic densities

The solution of the inverse gravity problem for determination of density anomalies from given potential anomalies is considered by H. Moritz under some conditions. In particular, the distribution of density is taken as a continuous function, which can be approximated uniformly by means of a system of polynomials. Then density, like the potential, can be expanded in series of spherical harmonics by polynomials (harmonic density). The other boundary condition is that a general solution, which corresponds to the zero-potential densities, is determined. That is such a distribution of positive and negative densities, which do not change the external gravity potential, as their total mass should be equal to zero. Anomalous harmonic densities are obtained by excluding the general solution from the harmonic densities.

Practically, it is considered not to be the general geopotential (normal plus anomalous), but the disturbing (anomalous) potential, which expansion is well known in the global scale by a conventional gravity model, such as EGM96. Therefore, the anomalous harmonic densities can be calculated using spherical harmonics of the disturbing potential. The following final algorithm from [2] was used:

$$\rho_h = \sum_{n=2}^{z} \sum_{m=0}^{n} \frac{M(2n+1)(2n+3)}{4\pi R^{n+3}} \times r^n (c_{nm} \cos m\lambda + s_{nm} \sin m\lambda) P_{nm}(\cos\theta),$$

where, ρ_h – anomalous harmonic density;
M – mass of the Earth;
R – radius of the Earth (in a point, to which the value of a geopotential is referred);
r – radius-vector of an internal point, in which a density disturbing the geopotential is determined;
$P_{nm}(\cos\theta)$ - Legendre polynomial of n^{th} degree and m^{th} order;
θ - central angle or spherical distance between R and r;
c_{nm} and s_{nm} – coefficients of the surface geopotential spherical harmonics.
Transformation of the external spherical harmonics to the internal spherical harmonics is implemented by this algorithm.

Estimation of the depth of disturbing layer by the number of harmonics

The obtained above density anomalies are obviously situated in different depths. Therefore the following question remains: which layers of the Earth are responsible for disturbance of one geopotential anomaly or another?
In our method an assessment of the disturbing layer's depth is computed by a known harmonic function in the geoid theory [3] for the case when the external potential of the internal masses confined by a sphere is determined

$$\frac{1}{\ell} = \sum_{n=0}^{\infty} \frac{r^n}{R^{n+1}} P_n(\cos\theta),$$

where ℓ - distance between point, to which the value of a geopotential is referred and point, to which the density disturbing the geopotential is referred.

Calculation was carried out with $n_{min}=2$. At the right part of the expression the normalizing coefficient of spherical functions $(2n+1)^{1/2}$ was used [6]. If $\theta = 0$, then $P_n(\cos\theta) = 1$ for any n, and ℓ = R-r. Under these conditions and for given values of ℓ, r and R the corresponding values of n were calculated.
Relationship between harmonic degrees n and depths ℓ of disturbing layers is shown in the bilogarithmic diagram (Map 4).
The software was developed within the gravimetric tomography method and allows to compute values of heights of both the full geoid (all harmonics of a model used) and differential geoid, values of the anomalous harmonic densities in units of g/cm^3 and values of upper cover depths of disturbing layers of the Earth. The spherical coefficients of the EGM96 global geopotential geoid model were used.
Characteristics of the global geoid height model's spherical harmonics are the input data for the method. They are both used for determination of the layers' depths disturbing geopotential and for computing of the harmonic dense anomalies. The spatial-scale of harmonics (half wavelength) or lateral resolutions of the EGM96 model is 0.5°. Maximum degree of the model is 360. Computing was carried out with an interval of 0.25°. Blue color indicates regions of less dense structures and yellow color indicates more dense structures in all figures below. On the other hand, density anomalies up to depths of about 100 km in isostatically compensated regions (mid-ocean ridges, abyssal basins et al.) are represented with a reversed sign so that to satisfy the isostatic geoid anomalies by equation $\Delta N = -2\pi G/g \int_0^h y \Delta\rho(y)dy$ [27]. In other words, a color scale for deep density bodies in images are interpreted on the contrary, namely: blue color indicates regions of more dense structures and yellow color indicates less dense structures.

I.2 ***Geoid topography by the EGM96 geopotential model*** 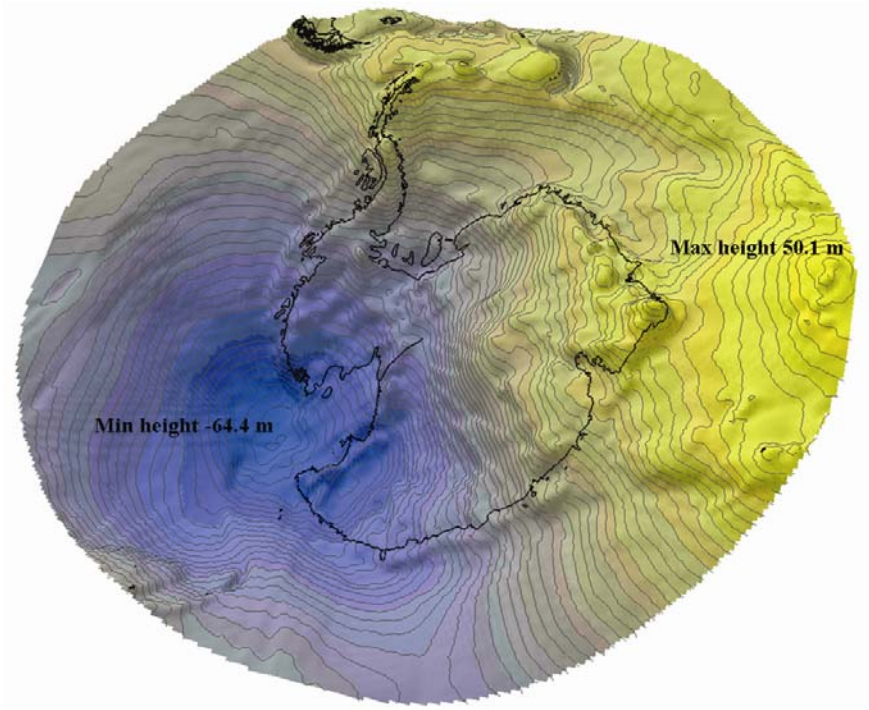	**I.2** ***Geoid topography by the EGM96 geopotential model*** **Geoid topography by the EGM96 geopotential model (Fig. I.2). Only two main structures have been discovered in the region. Epicenters of the structures correspond to known geoid undulations. One of them is the Antarctic undulation depression (-64.4 m) located near the Ross Sea and another one is the Conrad undulation with an elevation (+50.1 m) placed towards the Conrad Rise in the Indian Ocean [7].**

I.3 ***Differential geoid topography due to the disturbing layer of 50 km thickness***

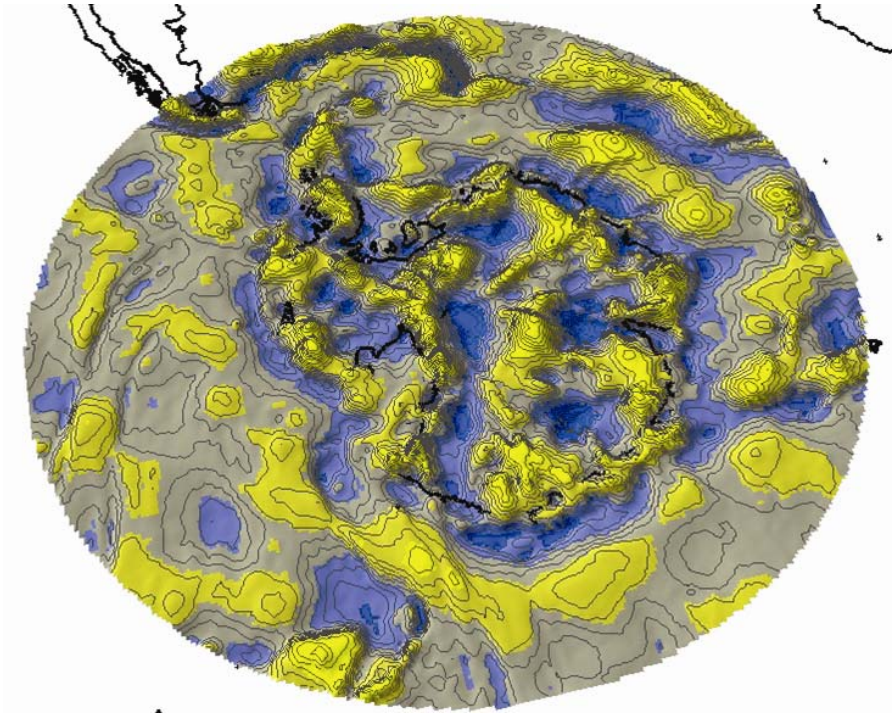

I.3 ***Differential geoid topography due to the disturbing layer of 50 km thickness***

The well-known extracting procedure of certain harmonics for determination of a residual (differential) geoid and for mapping of the structures in different layers, which disturb the geopotential was used. The differential geoid topography due to the disturbing layer of the 50 km thickness from the Earth's surface is shown in Fig. I.3. The relief of the Antarctica continent does not have an ice sheet and is co-ordinated with the BEDMAP topography [8].

II Interaction of Antarctica with other regions

II.1 *Distribution of dense (yellow) and thinning (blue) structures at a depth of 5300 km*

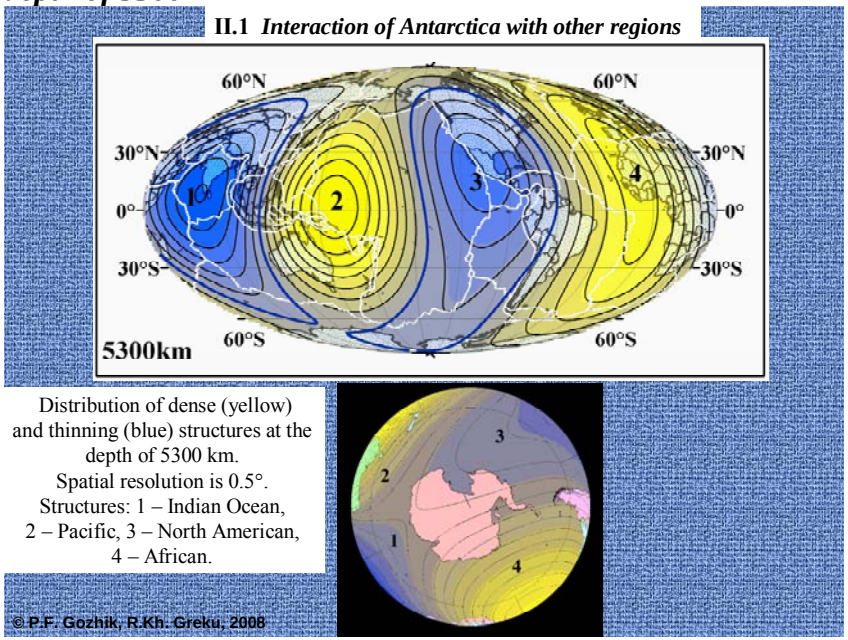

II.1 *Distribution of dense (yellow) and thinning (blue) structures at a depth of 5300 km*

A distribution of the global dense inhomogeneities is shown on the Map of the lateral slices at depths of 5300 (Maps 7, 8). Four structures are located almost symmetrically in the Earth's body on the inner core surface at the depth of 5300 km. It is shown that "1" and "2" structures have most anomalous values in the epicenters (-1.4-5 and 1.37-5 g/cm^3 accordingly), take similar areas and have the largest gradients between them (100°E-120°E) on Earth. Locations of the structures coincide with the geoid undulations (-102 m and 73 m) and the gradient zone is known as a region of catastrophic eruptions (Krakatau), earthquakes and tsunamis (e.g. 2004).

"3" and "4" structures have less values of density in their epicenters, but as against the "1-2" structures, they are extended for more regions and, what is important - they reach the Antarctica. Thus, masses of "3" and "4" structures are defining for the constitution and geodynamics of the Antarctic region at large depths and hinder extension of "1" and "2" structures. It is better visible in another projection on Figure below, where a convergence of four structures is shown. A symmetrical influence of each structure is apparently a reason for the stable location of the Antarctica continent during the breakup of the Gondwanaland in contrast to other continents.

II.2 ***Distribution of global dense inhomogeneities at a depth of 5300 km in the Lambert projection***

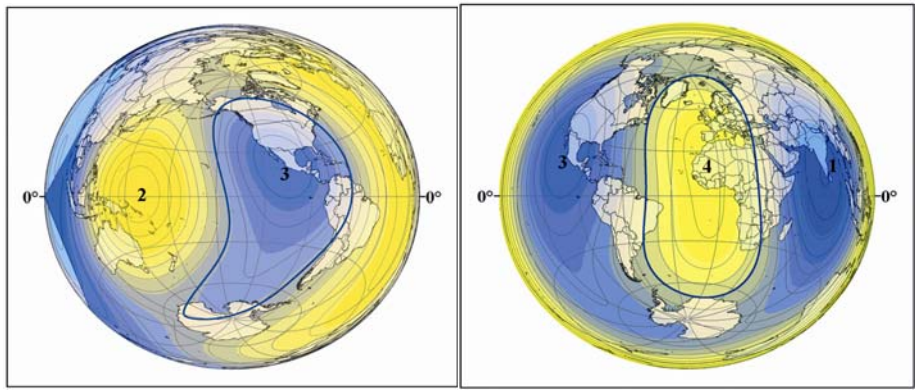

II.2 ***Distribution of global dense inhomogeneities at a depth of 5300*** **km** ***in the Lambert projection***

The spatial expansion of the “3” and “4” structures connected with Antarctica directly is visible more definitely in the Lambert projection. The figure “a” shows an initial connection of the West Antarctic with the North American structure at the depth of 5300 km. Its epicenter is in the area of the Columbia River relict plume (Murphy et al., 1998). The thinning masses of the plume in the area of the Ross Sea are localized at the depth of 2800 km as the “5” self-dependent structure (next page). It coinsides with the known Antarctic depression of the geoid about -64 m.

Masses of the “4” dense structure at the depth of 5300 km reach Antarctic also (Figure b). The localized part of the “4” at the depth of 2800 km southeastward of Africa, and named as the “6” structure, is connected with the East Antarctic (next page).

II.3 *Distribution of dense and thinning structures at depths of 5300 km, 2800 km and 1500 km*

II.3 Distribution of dense (yellow) and thinning (blue) structures at depths of 5300 km, 2800 km and 1500 km.

Spatial resolution is 0.5°.
Structures: 5 – Ross plume, 6 – South African.

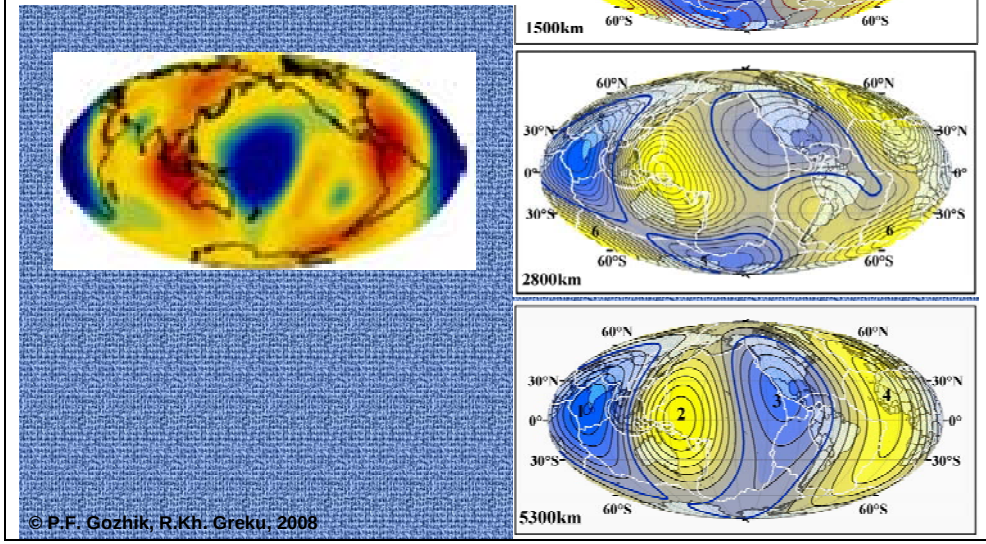

II.3 *Distribution of dense and thinning structures at depths of 5300 km, 2800 km and 1500 km*

The masses in the Antarctic area are detached from the maternal "3" and "4" structures (Map 7) and localized as the independent structures in the Ross Sea area ("5", 2800km) and to the South of Africa at 29°E ("6", 2800km, 1500 km). The "5" structure (Ross plume) is the most active in interaction with other dense (yellow) structures, in higher layers also. The structure "6" (South African) is represented as the root system of the Southwest Indian Ridge and the Southeast Indian Ridge and the Prince Charles Mountains at the Antarctic continent in the area of the Mackenzie and Prydz Bays.
There is a comparison with the seismic tomography model by Ishii and Tromp 2004 [9] shown at the left. But, the color scale is an inverse of the gravimetric tomography data, namely blue indicates regions where the relative perturbation is higher than average and red indicates values that are lower than average.

II.4 ***Distribution of dense anomalies along the Earth's axis of revolution between the North and South Poles***

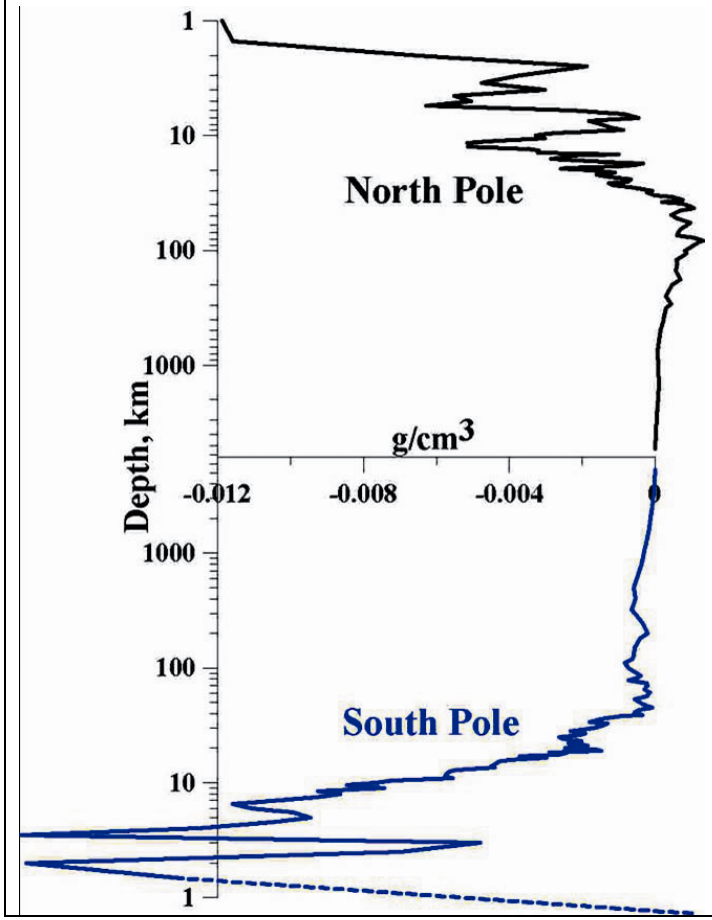

II.4 ***Distribution of dense anomalies along the Earth's axis of revolution between the North and South Poles***

Symmetry on the South Pole is violated significantly due to the presence of the Antarctic continent and an increase in anomalous density in upper layers.

III Transformation of the Earth's structure in different depths within the Antarctic lithosphere plate

III.1 *Lateral slices of anomalous dense inhomogeneities at depths of 1500 km, 467 km, 118 km and 59 km*

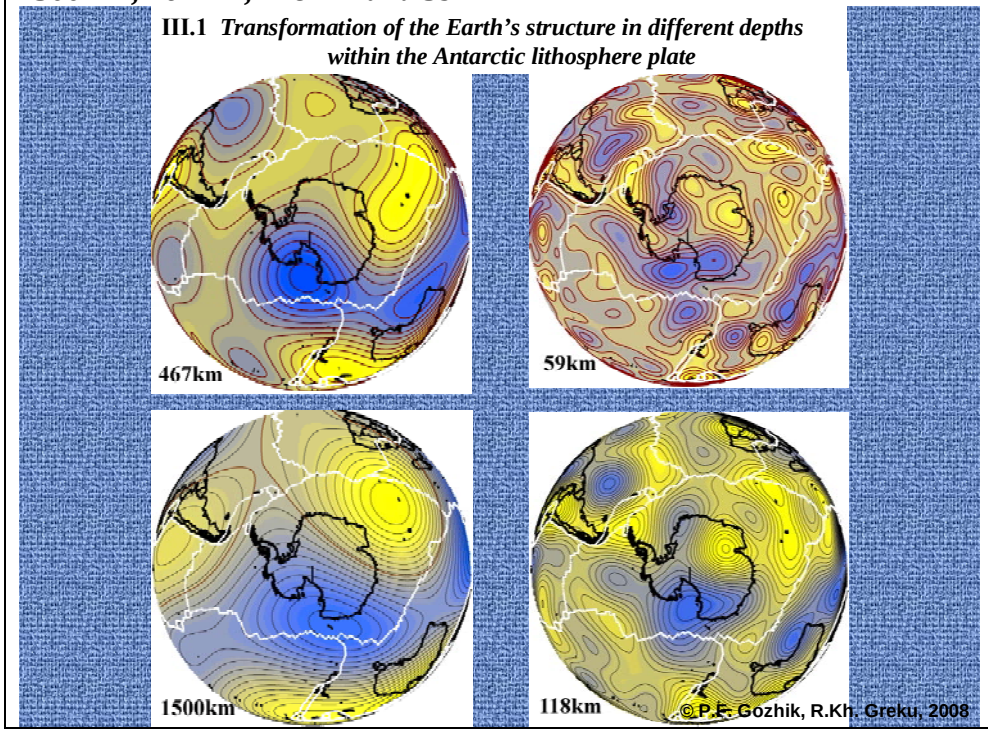

III.1 *Lateral slices of anomalous dense inhomogeneities at depths of 1500 km, 467 km, 118 km and 59 km*

Lateral slices of a distribution of anomalous density inhomogeneities in different discrete depths. White lines are boundary ridges between lithosphere plates. Maps are in the polar stereographic projection within the latitude of 30°S.

It is noted, that the Antarctic lithosphere plate within the limits of the boundaries of the ridges appears at depths about 118 km.

III.2 ***Lateral slice at a depth of 22 km***

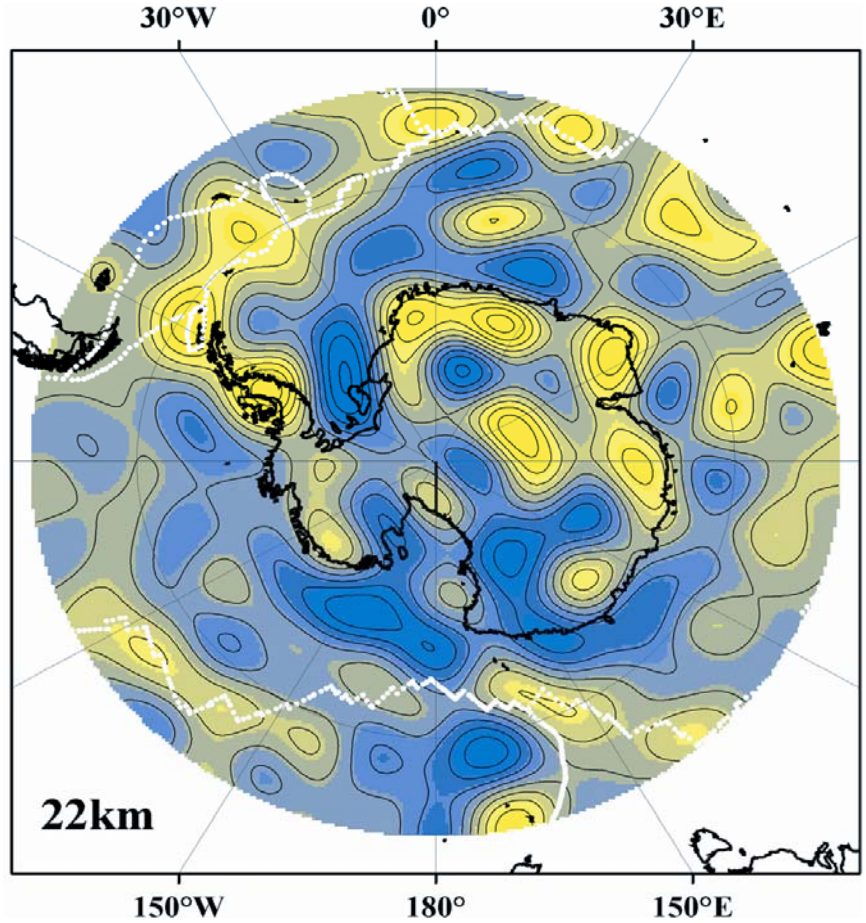

III.3 ***Lateral slice at a depth of 10 km***

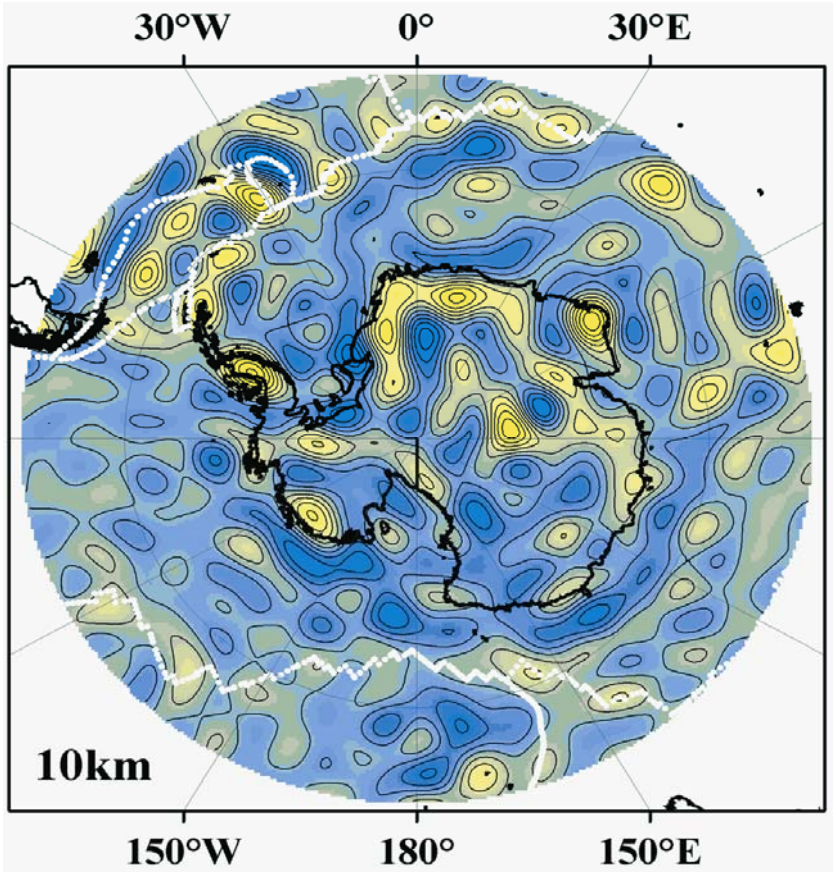

III.4 ***Lateral slice at a depth of 5 km***

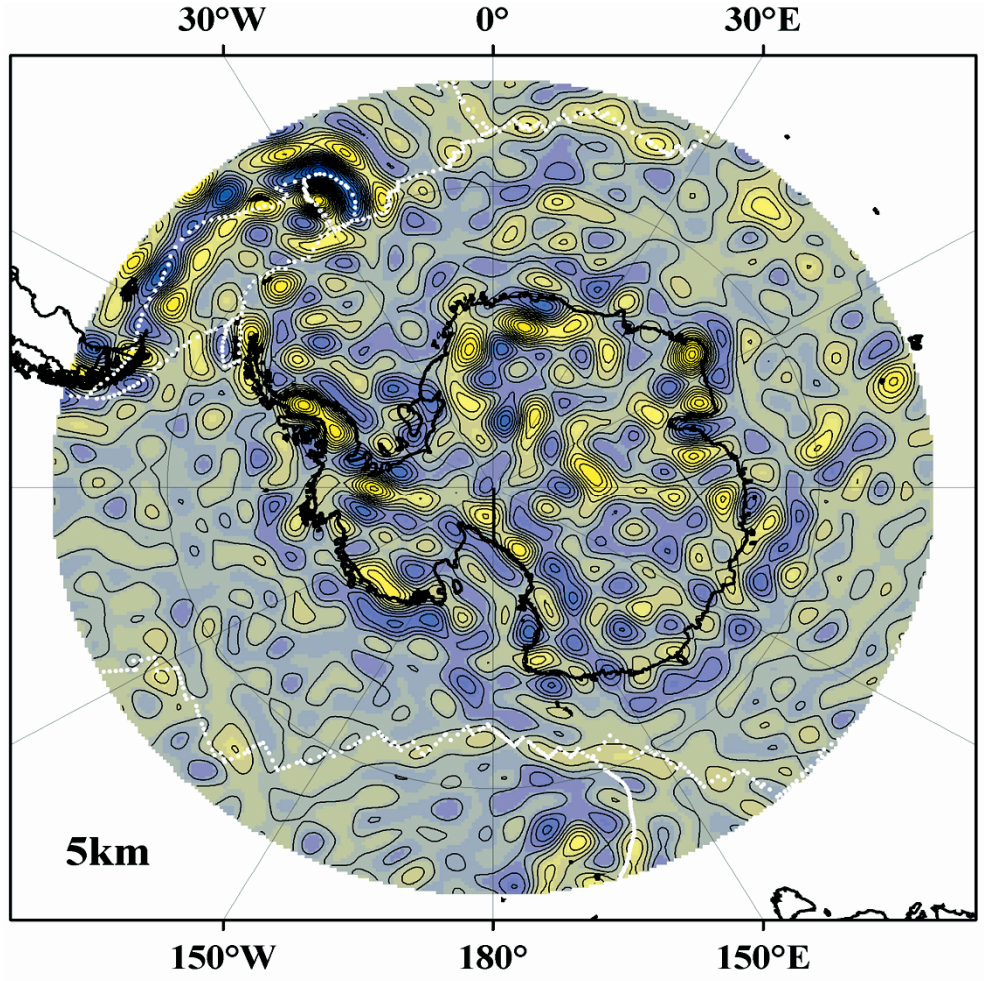

III.5 ***Lateral slice at a depth of 0.7 km***

There is a radial distribution of structures with the centre at the South Pole [10]

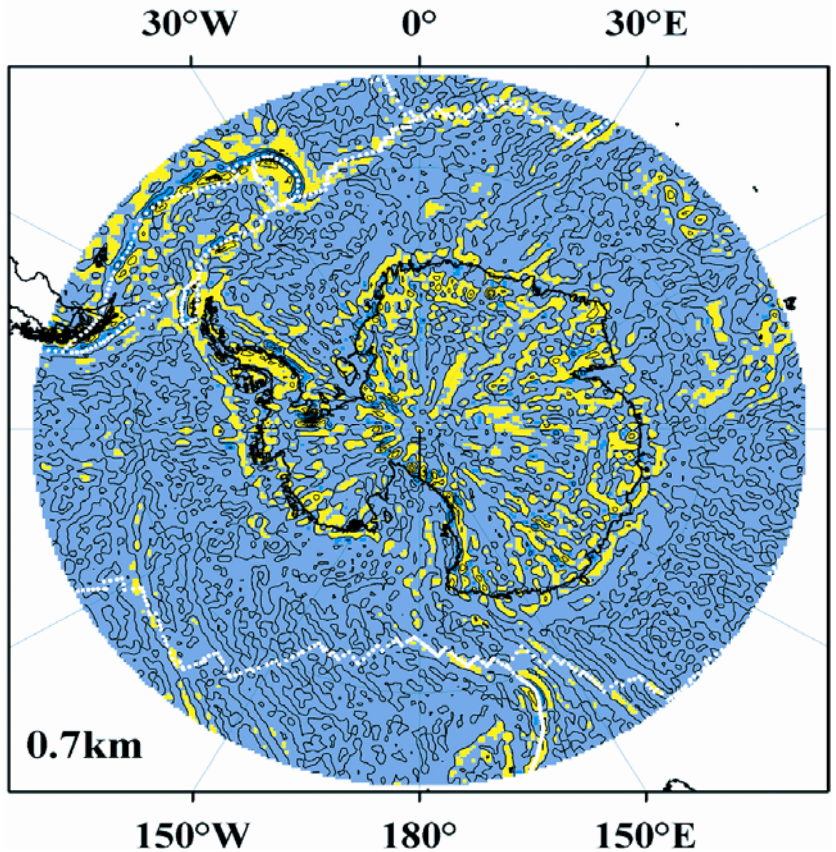

IV Antarctic lithosphere boundary

IV.1 *Deep structure of the Antarctic Plate boundary zone*

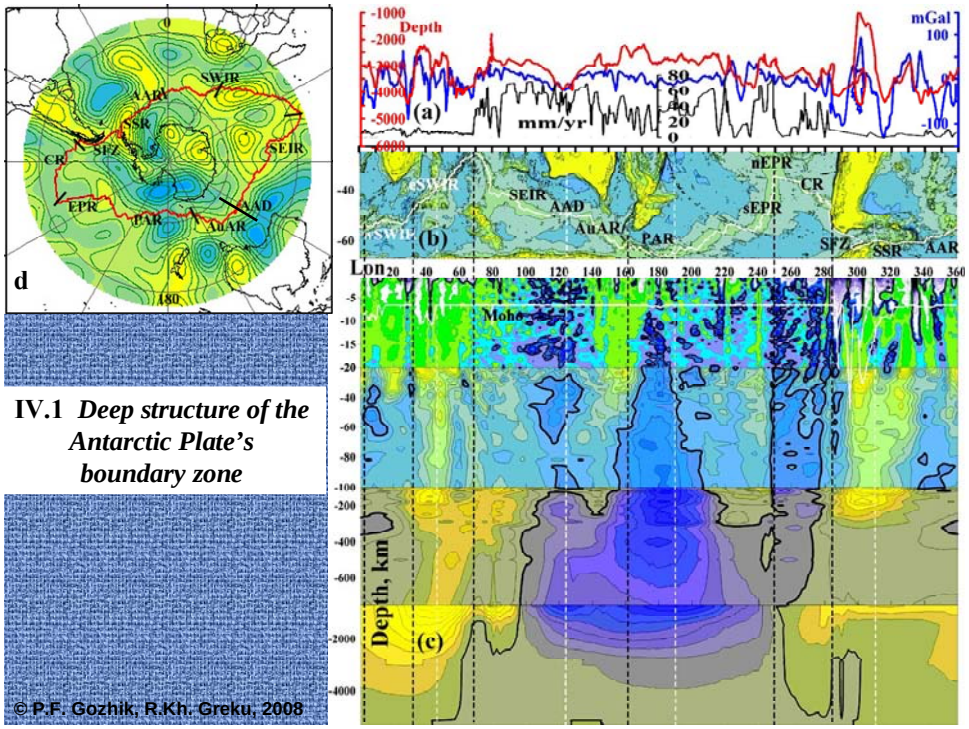

IV.1 *Deep structure of the Antarctic Plate's boundary zone*

IV.1 *Deep structure of the Antarctic Plate boundary zone*

The Antarctic Plate boundary (APB) is a contact zone with segments of five other large plates (Africa, Australia, Nazca, Pacific, South America) and five small plates (Shetland, Scotia, Sandwich, Somalia, Juan Fernandez). The extent of the boundary is 40,311 km taking into account many of offsets and discontinuities of ridges in accordance with the PB2002 digital model [11].

The APB (red line in Figure "d") includes the following spreading ridges: Pacific Antarctic Ridge (PAR); East Pacific Ridge (EPR); Chile (or Nazca) Ridge (CR); South Scotia Ridge (SSR); Sandwich Ridge (SR); American Antarctic Ridge (AAR); western Southwest Indian Ridge (wSWIR); eastern Southwest Indian Ridge (eSWIR); Southeast Indian Ridge (SEIR); Australia-Antarctic Ridge (AuAR); Shackleton Fracture Zone (SFZ). Background data of the Map in Figure "d" displays a distribution of structures, which the harmonic density anomalies are relating to the PREM density model at a depth of 59 km.

Profiles of the bottom topography, the free-air gravity anomalies from KMS2002 [12] and a curve of spreading rates along APB [11] are shown in Figure "a".

APB against (white line) a background of the bottom topography and continents are shown in Figure "b".

Density inhomogeneities are displayed in Figure "c". The spatial resolution is 60 km along the APB. White dotted lines are positions of orthogonal to APB cross-sections and black dotted lines are locations of triple-junction points. The vertical exaggerations in Figure "c" are different for distinct layers (divided by horizontal lines).

The whole range of density anomalies values is between -0.0983 g/cm^3 and 0.0491 g/cm^3. The thick isoline marks the value of 0.0 g/cm^3. Two bodies (plumes) with maximum depths of near 2800 km on the core-mantle boundary dominate in the mantle. Less dense hot masses (blue tint) ascend upright and become as three branches from the depth of 200 km. One of them is directed towards AAD (124°E), another one - northward the Ross Sea (175°E) and third one to the boundary of the Nazca plate (250-280°E). An active penetration of the masses in the form of impulse drops is visible up to the surface in area of lengthening transform fault zone of the Chile Ridge. It apparently causes an accelerated spreading process [13]. Dense masses (yellow tint in area of 50°E) are apparently cold relict plume (Conrad-Del Cano), which was shaped under Gondwanaland and then was involved in the process of separation of the Antarctic block from other continents [14].

IV.2 ***The Australian-Antarctic Discordance (AAD) anomalous structure***

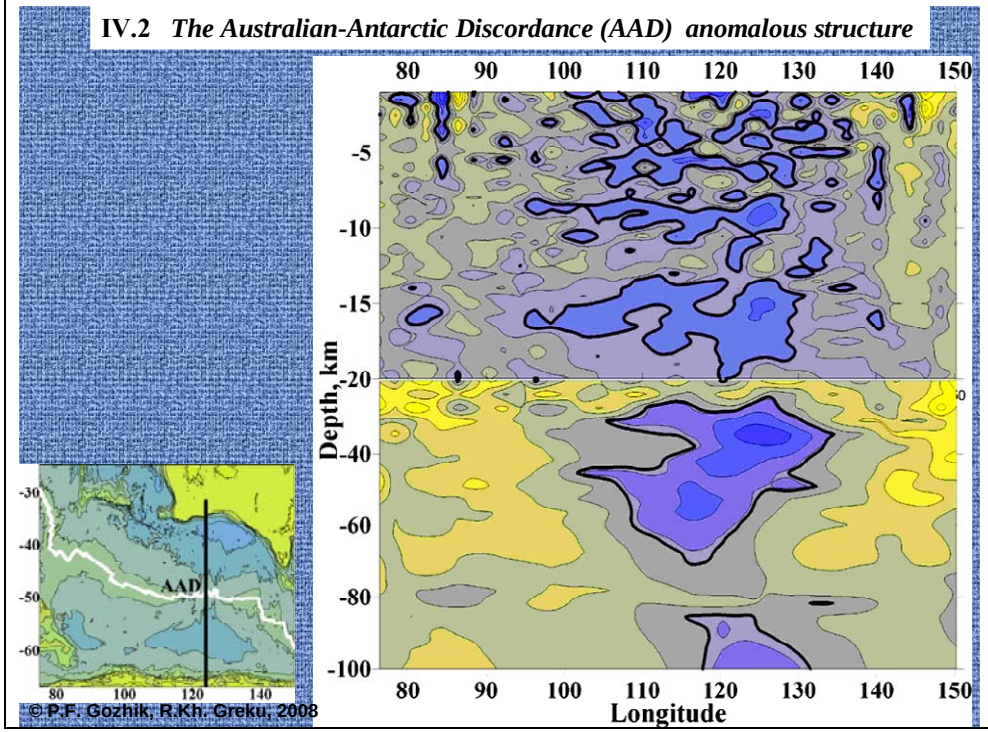

IV.2 ***The Australian-Antarctic Discordance (AAD) anomalous structure***

The rising of the plume fluids is discovered from the depth of 150 km in the AAD region. It is seen that thinning hot masses penetrate into the colder oceanic crust and lithosphere.

IV.3 ***Vertical cross-section of dense heterogeneities along the meridian of 124°E crossing the AAD***

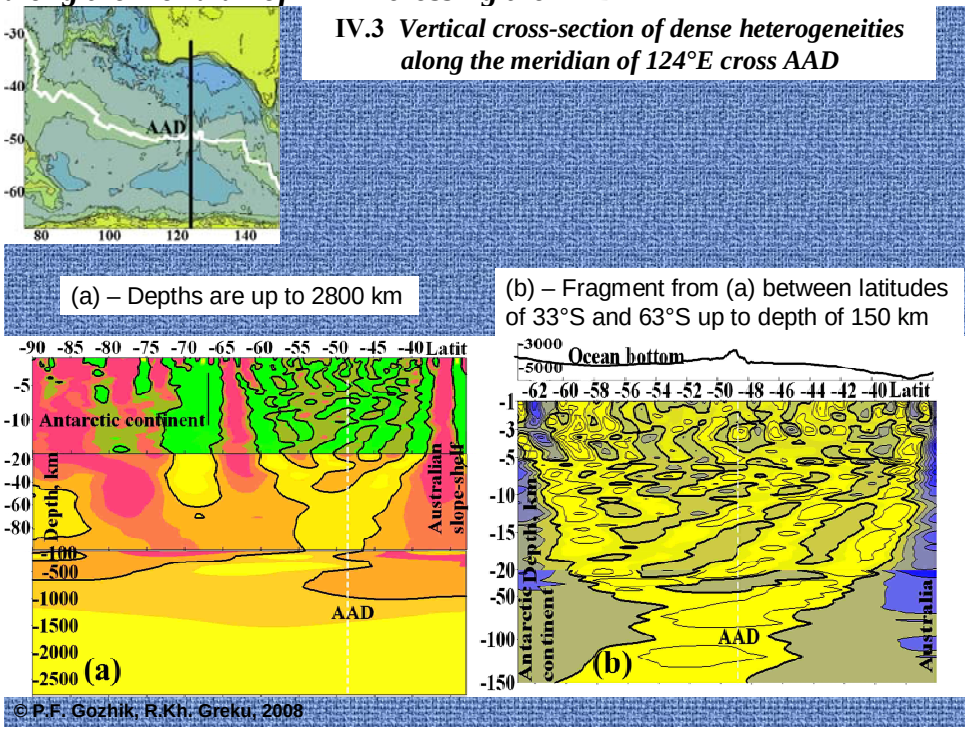

IV.3 ***Vertical cross-section of dense heterogeneities along the meridian of 124°E crossing the AAD***

Meridian section along 124° E. The ascending masses of the AAD hinder to join SEIR and AuAR at the interval of 110°E-135°E (Map 16). The root parts of SEIR and AuAR are diverged southward and northward accordingly on the lateral Maps at depths of 50 km, 30 km and 10 km. It is the result of an infiltration of the plume material into the AAD area from depths of 50-60 km (Figure "a", "b"). The area between slabs in Figures "a" and "b" is characterized by an active intrusion of the plume thinning masses. A curved form of dense structures at the right south part in Figure "a" supposes an abrupt displacement of the ocean crust up to depths of 5-6 km northward from the Antarctic continent. At the same time, an active displacement southward is obvious at larger depths from 20 km up to 1200 km (Figure 3a). Such scheme of the interplate interaction can be an answer to the question in the ANTEC/SCAR (Lithosphere Structure & Stress) materials (www.antec.scar.org): "How to resolve the geodynamic paradox: Antarctica is surrounded by spreading centres but shows extensional features and low seismicity?"

IV.4 *Detailed fragment of the APB within the American-Antarctic and the Africa-Antarctic Ridges*

IV.4 ***Detail fragment of the APB within the American-Antarctic and Africa-Antarctic Ridges***

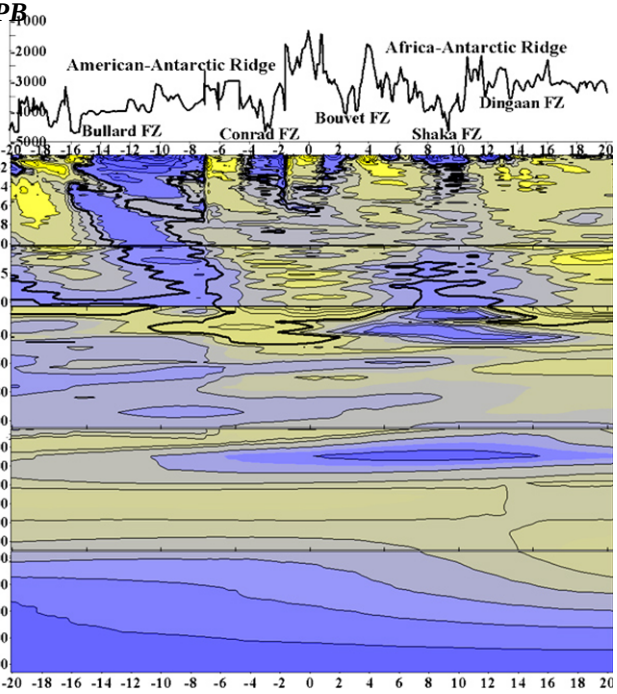

MAR – Mid Atlantic Ridge,
B – Bullard Fracture Zone,
C – Conrad FZ, B I – Bouvet Islan
Sh – Shaka FZ, D – Dingaan FZ

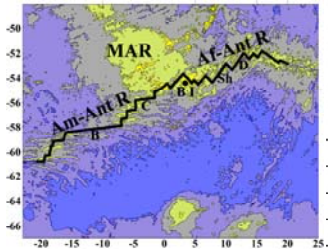

V Trans Antarctic vertical sections

V.1 *Scheme of the sections*

Position of the vertical sections crossing the Antarctic lithosphere plate

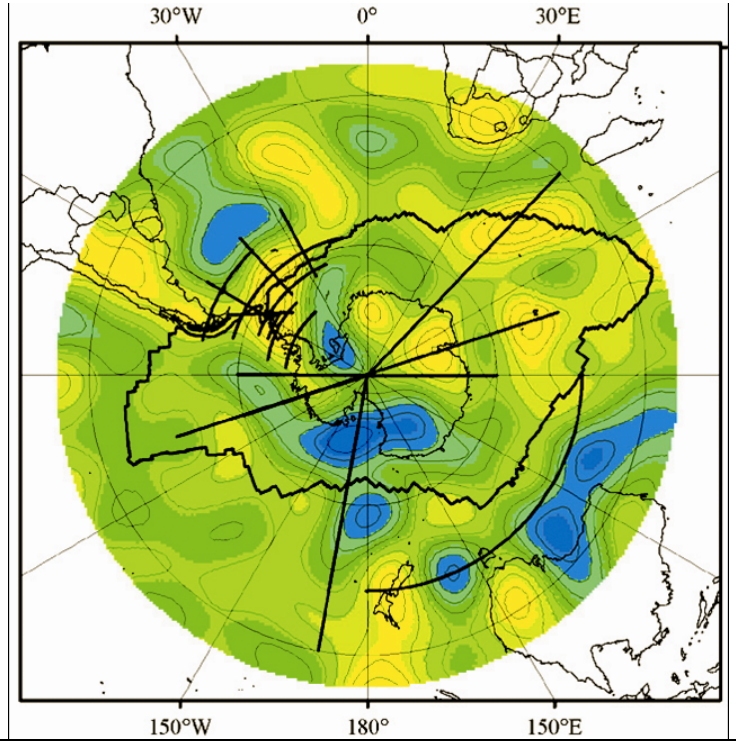

V.2 *Section along meridians of 190°E - 44°E. Range of depths is 140–2800 km*

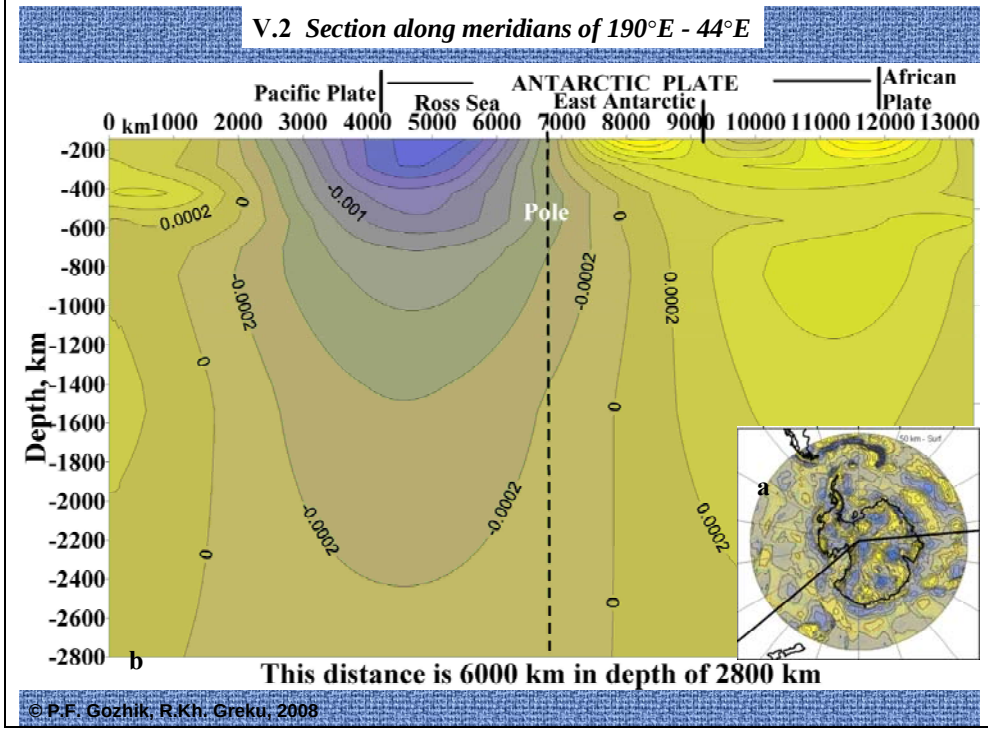

V.2 *Section along meridians of 190°E - 44°E. Range of depths is 140–2800 km*

a - Map of the differential geoid topography. The thickness of the disturbing layer is 50 km from the terrestrial surface and ocean bottom. Contour interval is 1.0 m. Solid lines show locations of the cross-section along directions of 190°E-Pole-44°E between latitude 30°S.

b - A deep structure of the region is shown at the vertical two-dimensional cross-section. An extension of the section is 13.365 km. An interval between calculated points is 30 km. This section crosses the whole Antarctic Plate between the Pacific-Antarctic Ridge (PAR), South Pole and South-West Indian Ridge (SWIR). It includes such geographical structures as the Pacific plate, PAR interplate boundary, epicenter of the Antarctic geoid negative undulation, West Antarctic Rift System (WARS), Polar zone, East Antarctica, Indian Ocean part of the Antarctic Plate, epicenter of the Conrad geoid positive undulation, SWIR and African Plate. Density inhomogeneities with the harmonic density anomalies are shown in g/cm^3. Contour interval is 0.0002 g/cm^3. Range of depths is 140 km – 2800 km. Three large-scale zones with a different density are distinguished clearly. The central zone I is related to the Antarctic negative undulation with the lower dense masses. A range of the harmonic dense anomalies is 0 ÷ -0.002 g/cm^3. This zone is located at depths of more than 140 km and includes a part of the Pacific Plate, the West Antarctic between PAR and TAM. Zones of higher density are located on the right side of the figure (II, East Antarctic between TAM and SWIR, 0 ÷ +0.0015 g/cm^3) and on the left (III, Pacific Plate, 0 ÷ +0.0006 g/cm^3).

V.3 ***Section along meridians of 190°E - 44°E. Range of depths is 1–2800 km***

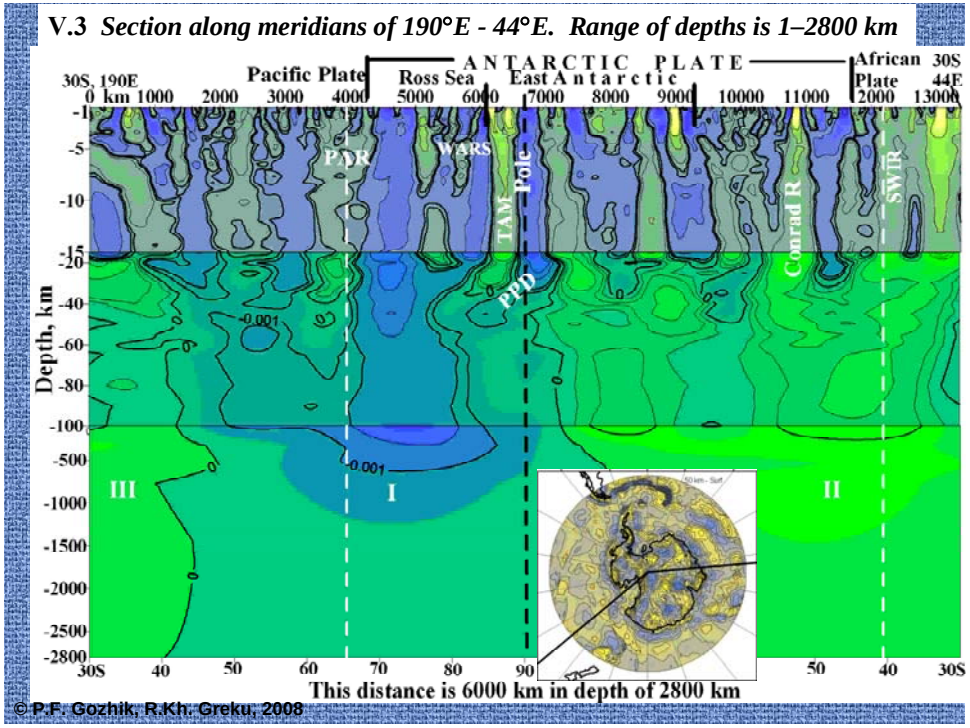

V.3 ***Section along meridians of 190°E - 44°E. Range of depths is 1–2800 km***

Vertical cross-section of density inhomogeneities with the harmonic density anomalies in g/cm^3 is located along 190°E and 44°E meridians through the South Pole between 30°S. Range of depths is from 1 km to 2800 km. PAR - Pacific-Antarctic Ridge, WARS - West Antarctic Rift System, TAM - Transantarctic Mountains, Conrad R – Conrad Rise, SWIR - South-West Indian Ridge. Vertical scales for the blocks in the depths of 1-15 km, 15-100 km and 100-2800 km are different. A tectonic interaction between the zones I, II and III and corresponding displacements of the contour lines can be seen in depths of 400-500 km, 600-650 km (upper and lower segments of the Benioff zone) and 1500 km. Gradients and a spatial differentiation of the anomalies increase closer to the surface.

V.4 ***Detailed image of the section along the meridian of*** **190°E** ***between latitudes of 60°S – 90°S***

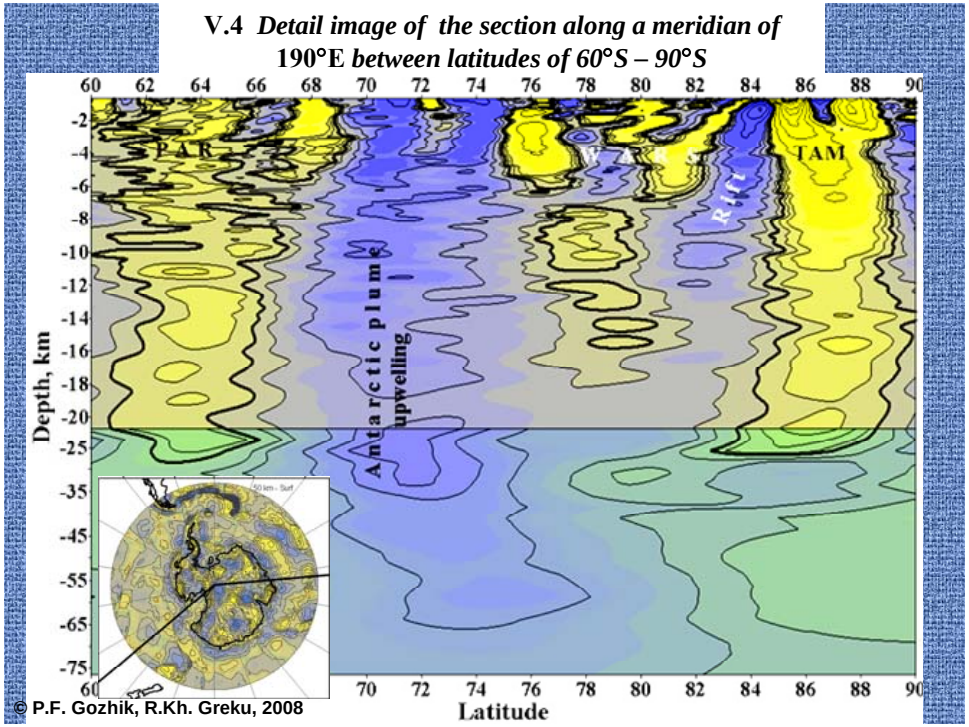

V.5 ***Detailed image of the section along the meridian of*** **44°E** ***between latitudes of 30°S – 90°S***

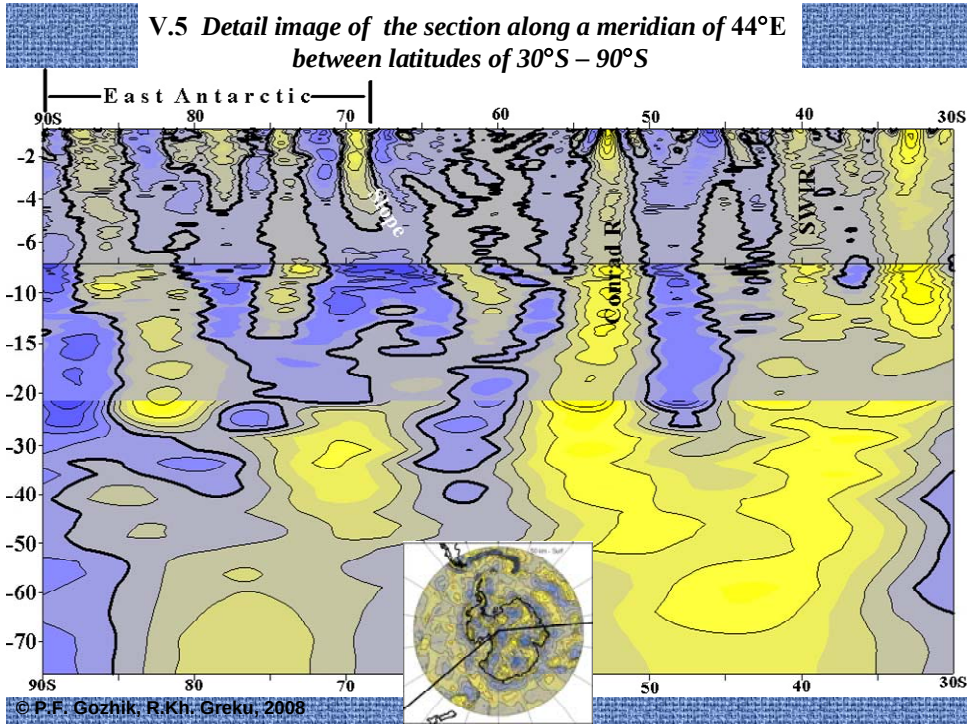

V.6 *Features of the West Antarctic Rift System*

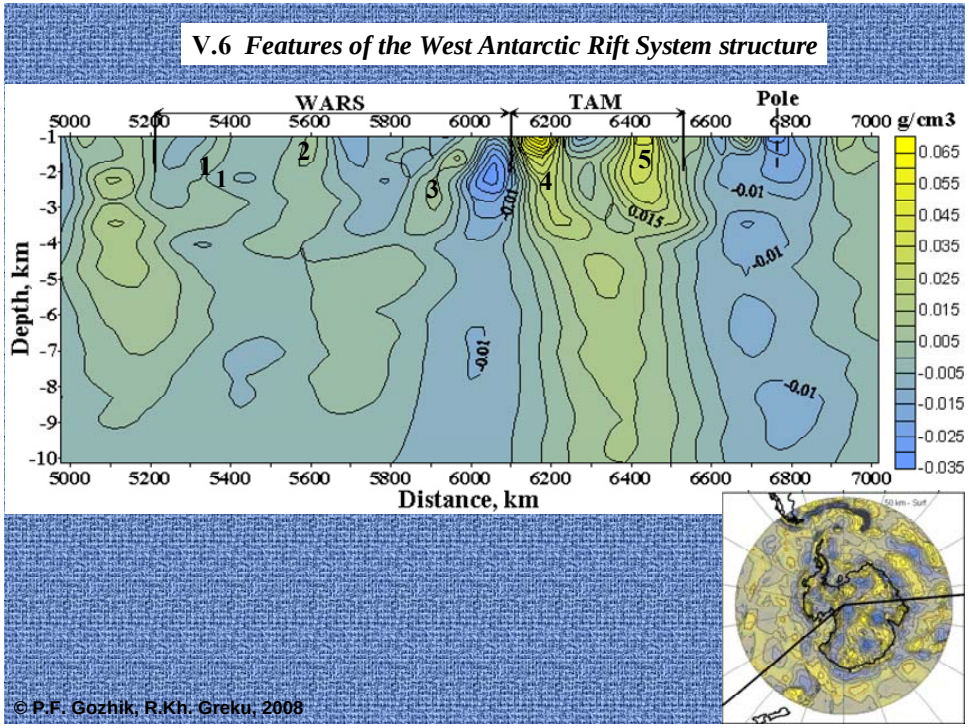

V.6 *Features of the West Antarctic Rift System*

Fragment from the cross-section in the previous Map 22 with the West Antarctic Rift System. Range of depths is 1 km – 10 km. 1-3 - spreading blocks, which float off the rift to the west; 4-5 – massif TAM to the east from the rift. Contour interval is 0.005 g/cm^3.

Two main channels of the lifting up of a material of the zone I from depths can be seen. One of them is located at a mark of distances of 4500 km in depth of 60 km. The second is at a mark of 6100 km and in depth of 20 km, the last is the actual rift. Besides, there is one more channel which is clearly seen to the east of TAM on a mark of distance of 7000 km. Its root is turned to the west and supports TAM from below at the depth of 50 km. Apparently, it also should be included into the WARS system.

The erupted cooled blocks with numbers of 1, 2 and 3 at the left and 4 and 5 at the right of the rift are floating off the rift in both sides and dipping with inclination up to 3.0-4,5 km. A distance of the blocks from the rift is not symmetric. For example, a distance between blocks of 1-3 is 200-400 km. At the same time the blocks 4 and 5 are united (welded) in to a single mountain system, which root is marked in depths more than 40 km.

V.7 ***Section along meridians of 90°W - 90°E***

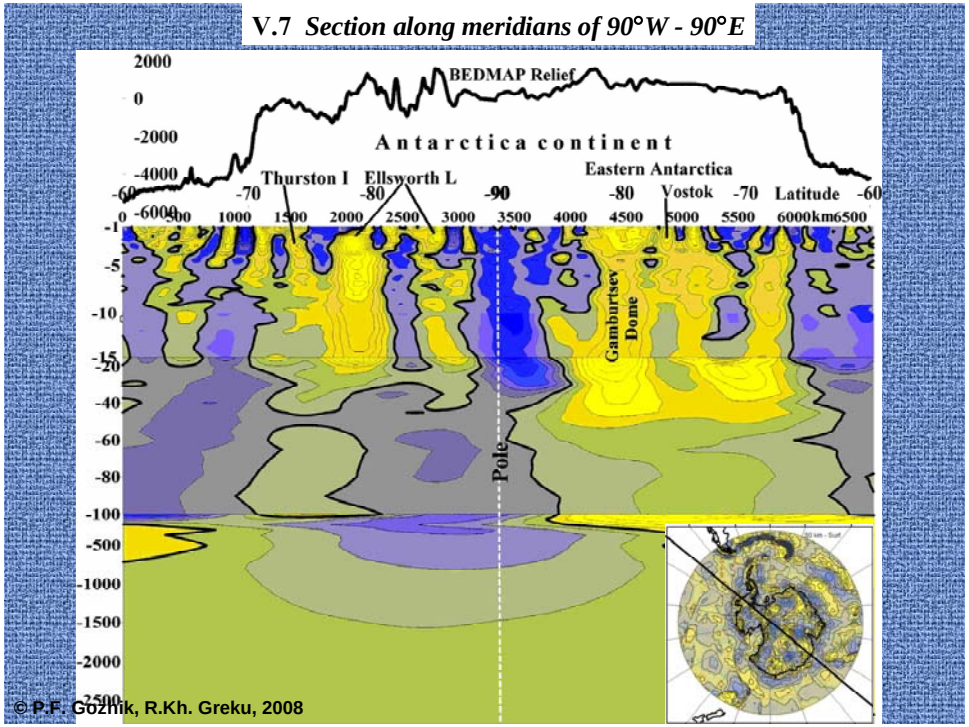

V.7 ***Section along meridians of 90°W - 90°E***

In the region of the Ellsworth Land there exists an evidently former rift channel as well, which is currently blocked at a depth of 25-30 km therefore does not remain active as noted in the paper [15].

V.8 *Section along meridians of 108°W - 72°E. Comparison between the gravimetric and seismic tomography data*

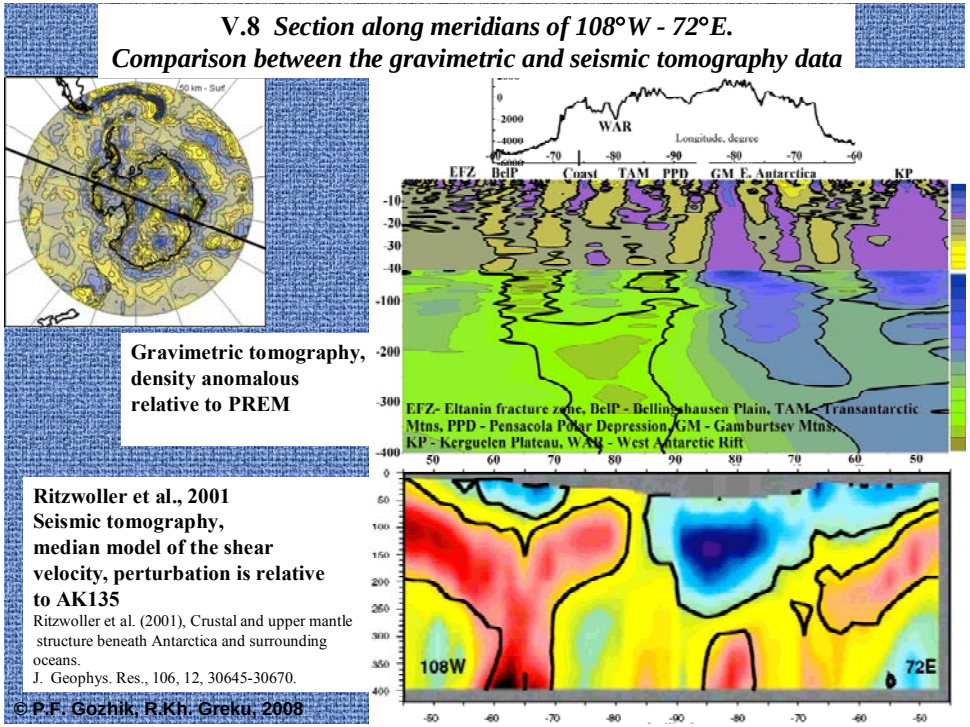

VI Sections crossing the West Antarctic

VI.1 *Section along 65.25°S crossing the Antarctic Peninsula (Graham Land)*

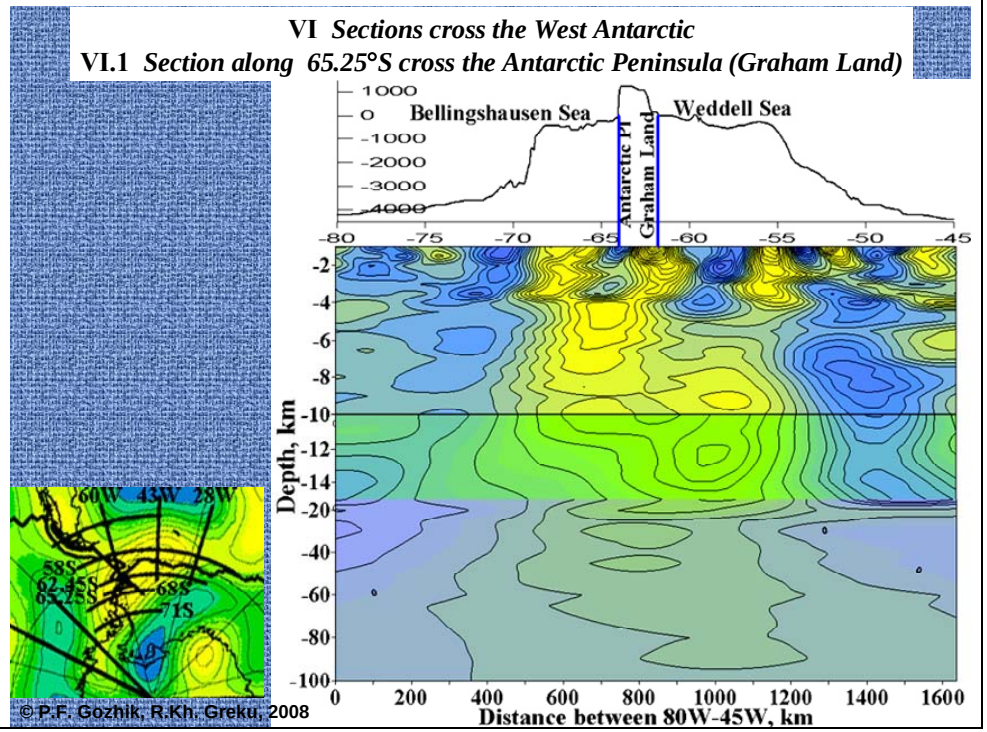

VI.2 *Section along 68°S crossing the Antarctic Peninsula (Transit Zone)*

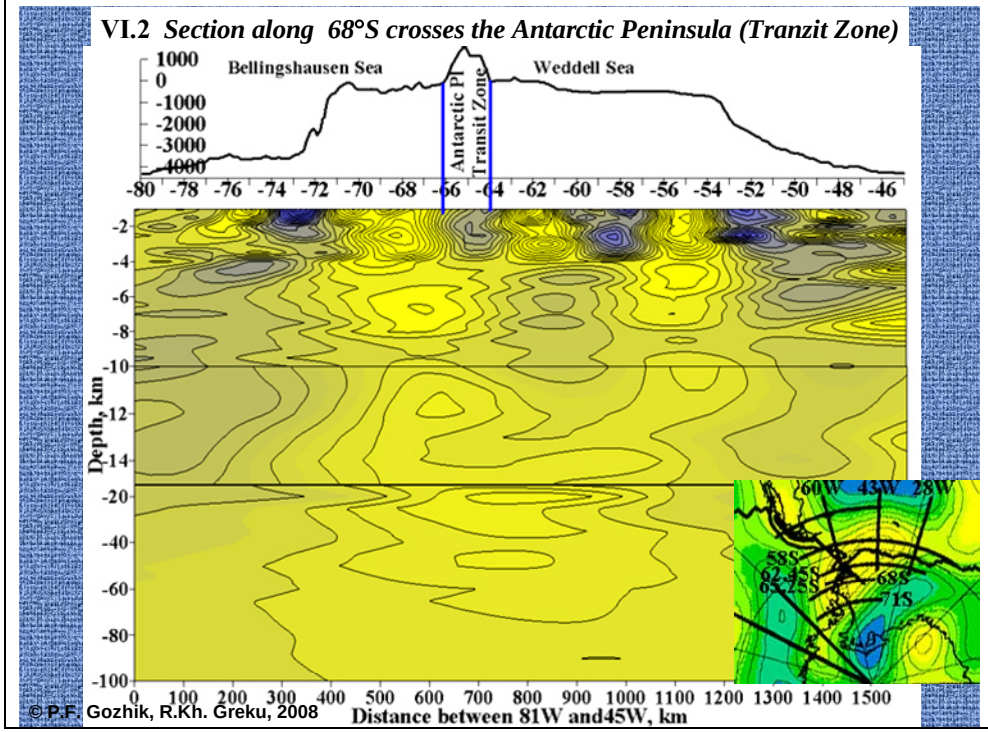

VI.3 *Section along 71°S crossing the Antarctic Peninsula (Palmer Land)*

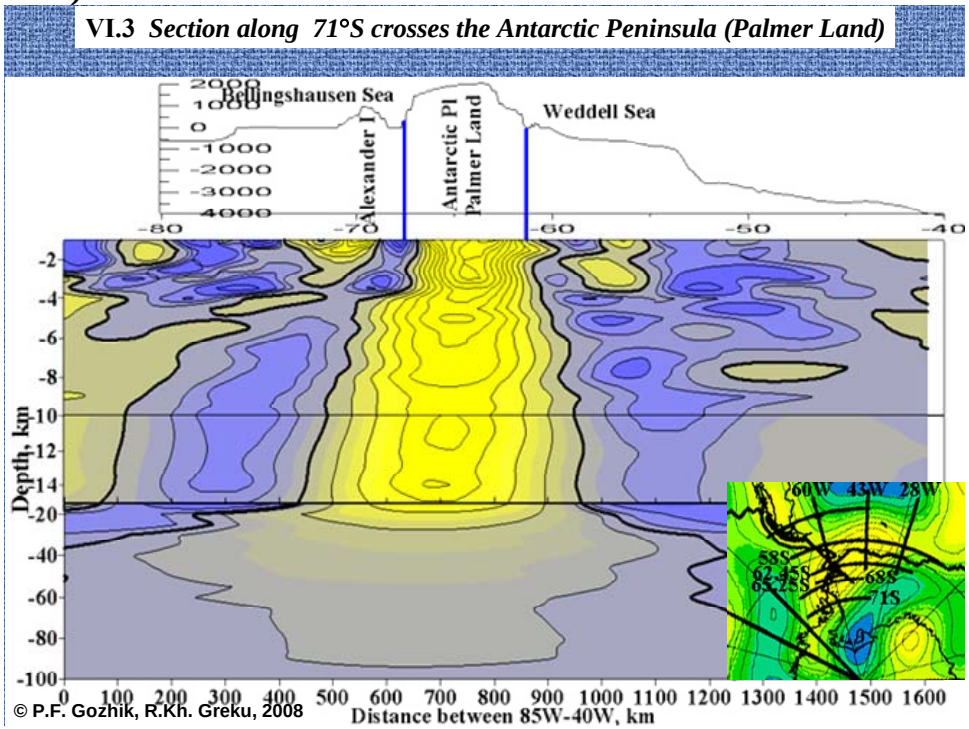

VI.4.1 *Section along the direction of Drake Strait-Deception I-Antarctic Peninsula-Weddell Sea*

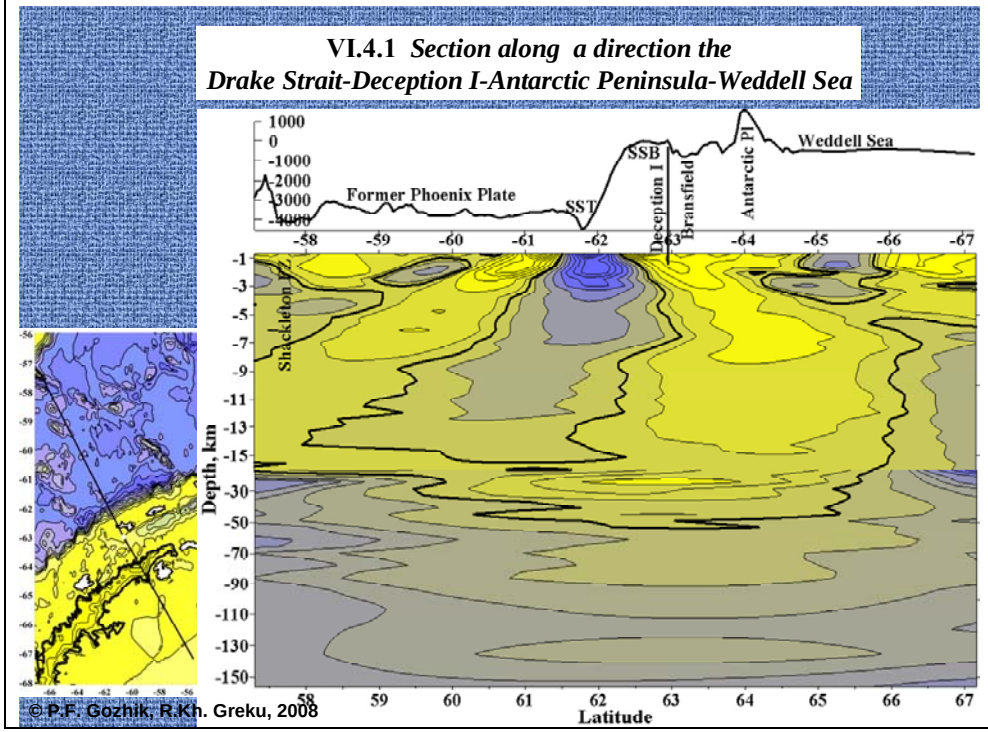

VI.4.2 *Section along the direction of Drake Strait-Deception I-Antarctic Peninsula-Weddell Sea. Depths are shown from the sea surface*

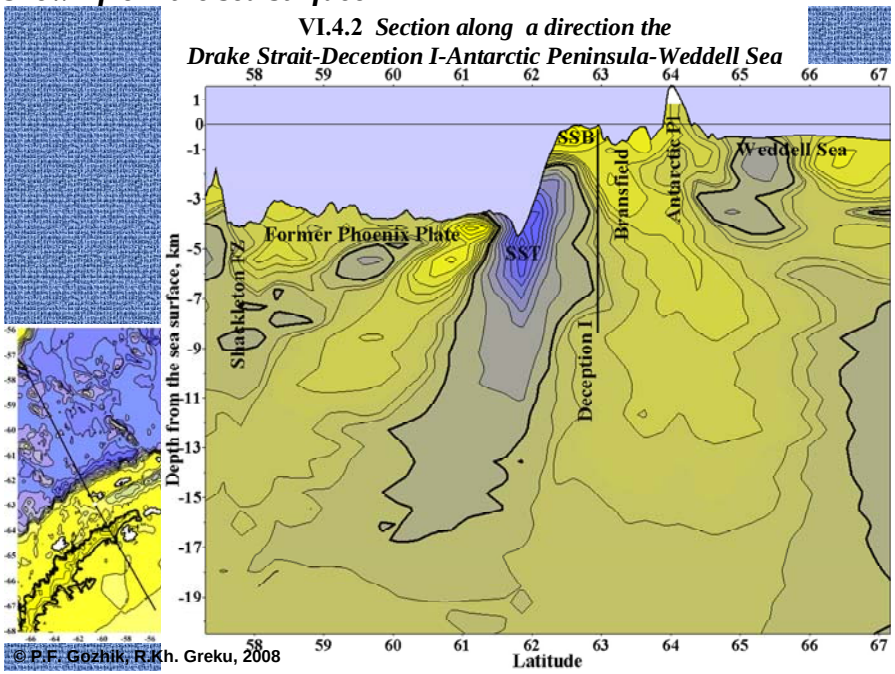

VI.5.1 ***Link of the Bransfield Basin with the Weddell Sea along 62.4°S***

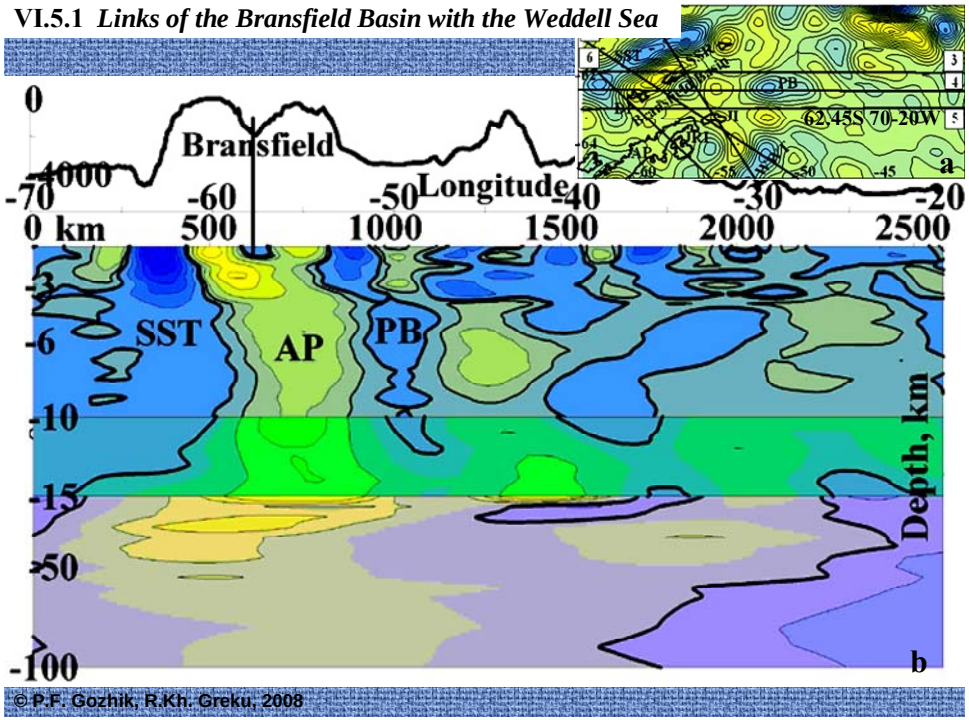

VI.5.1 ***Link of the Bransfield Basin with the Weddell Sea along 62.4°S***

a - Map of the vertical sections across the Bransfield Basin. Background is a distribution of dense heterogeneities at the depth of 1 km. AP – Antarctic Peninsula, DI – Deception Island, JI – Joinville Island, JRI – James Ross Island, PB- Powel Basin, SSR – South Shetland Ridge, SST – South Shetland Trench, WWT – West Weddell Trench. 1-6 – numbers of cross-sections.

b - Cross-section 5 of dense heterogeneities along 62.4°S between meridians 70W-20W up to a depth of 100 km (maximum anomalous values are -8-2 and 4-2).

It is seen that the root part of anomalous masses of AP is bent like an arc eastward under the influence of the Pacific crust spreading. This bend has a most distance of 130 km at depths of 7-8 km. The Bransfield Channel is moved to the east also. The main sources of thinning masses coming to the Bransfield Basin (BB) are in the Weddell Sea. The Powel Basin (PB) is a source discovered in Figure "b". The link of the PB's matter is visible at depths of 1.8-2.5 km between the distance marks of 680-800 km. Now it is closed apparently at the distance point of 711 km and at the depth of 2 km.

VI.5.2 *Link of the Bransfield Basin with the Weddell Sea along different cross-sections*

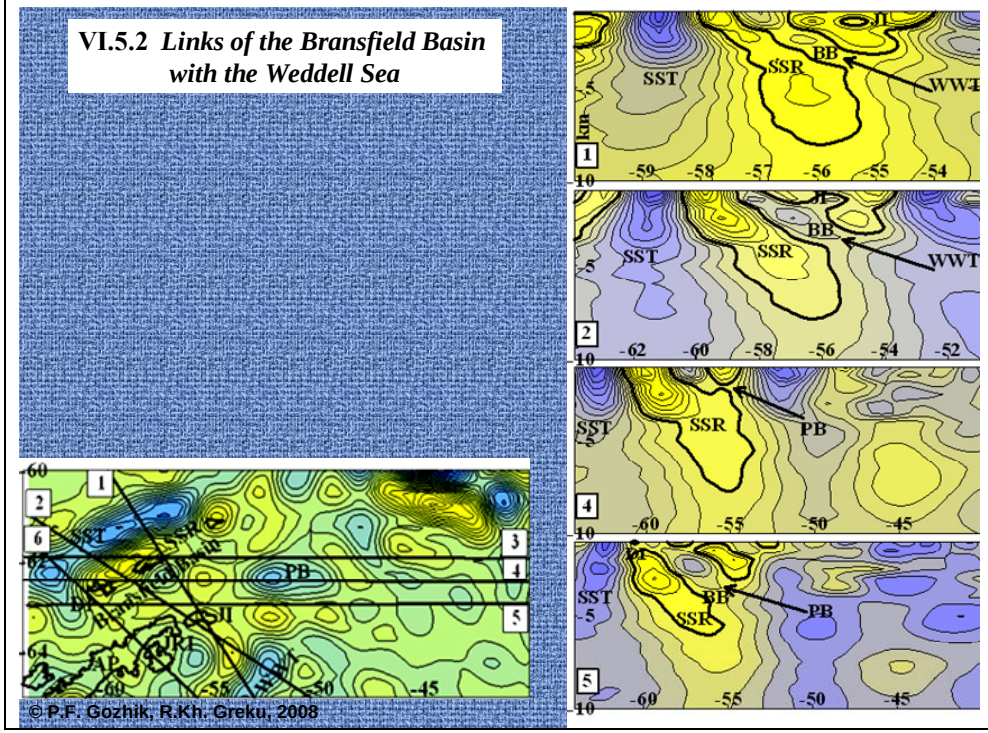

VI.5.2 *Link of the Bransfield Basin with the Weddell Sea along different cross-sections*

The deep channels between the Bransfield Basin and the Weddell Sea are discovered at other sections from another source. It is a structure located along the eastern slope of AP in area of 50°W (Figure "a"). It is a definite component of a subduction zone, like the South Shetland Trench [16]. It is called the West Weddell Trench (WWT) in this work. It is not visible in bathymetry but is disclosed clearly in the geoid topography and especially in the differential geoid as a difference between the detailed altimetric geoid and the OSU91 geoid model [17]. These examples confirm the supposition that the Bransfield rift merges eastward [16, 18].

VII Detailed structural maps of the West Antarctic

VII.1 *Density lateral slice at a depth of 5 km*

VII ***Detail maps of the West Antarctic***
VII.1 ***Density lateral slice at the depth of 5 km***

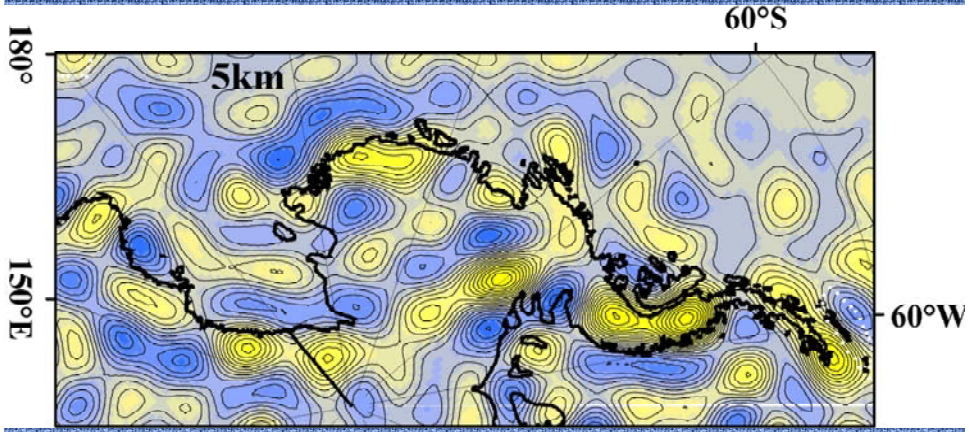

VII.2 *Density lateral slice at a depth of 0.7 km*

VII.2 ***Detail map of the West Antarctic with the density lateral slice at the depth of 0.7 km***

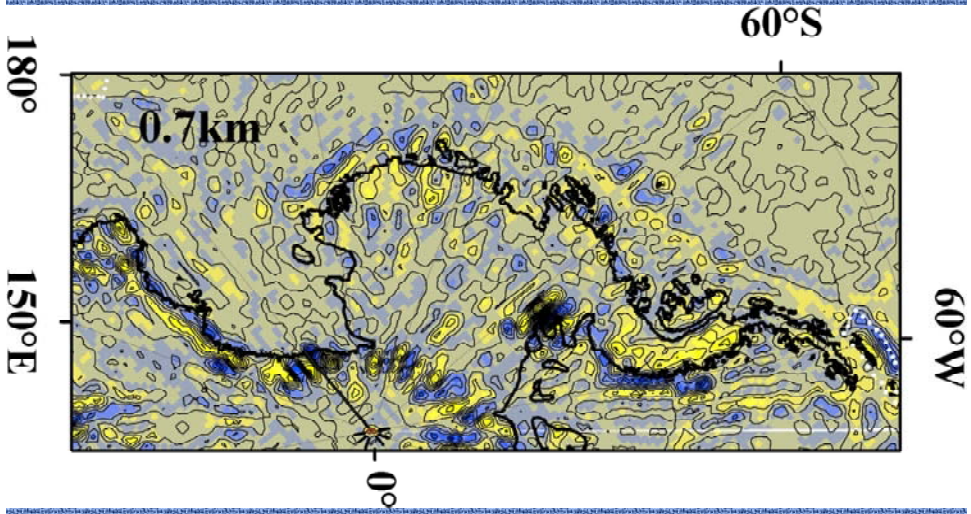

VIII Regional structural features of the Scotia Plate

VIII.1 *Distribution of dense heterogeneities along the central latitude of 58°S between depths of 1-100 km*

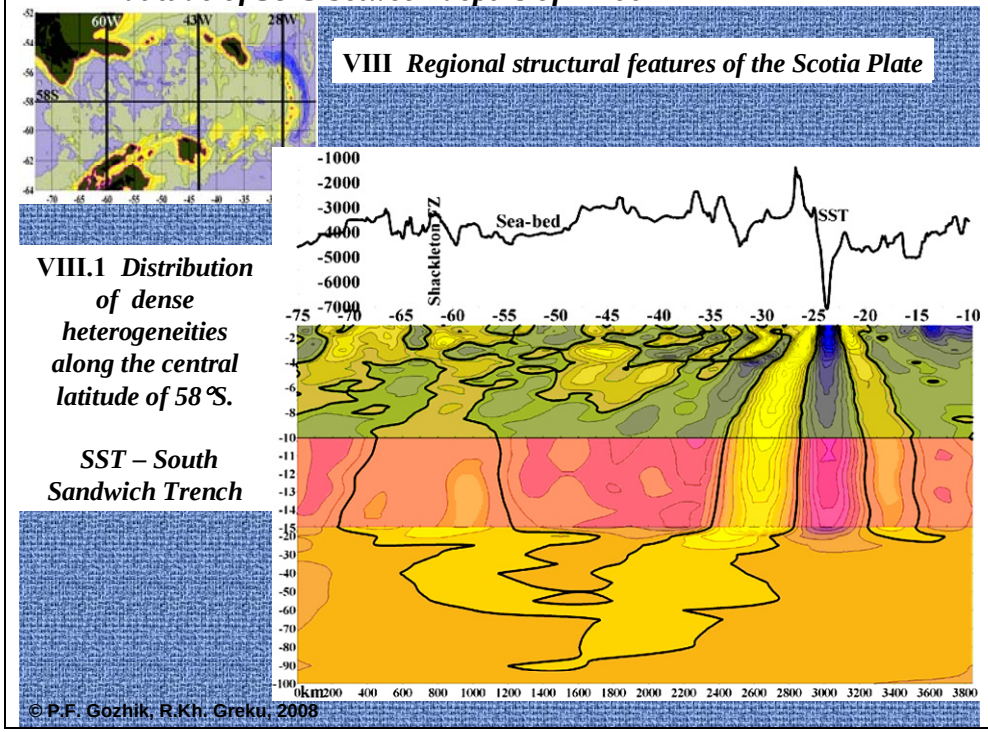

VIII.1 ***Distribution of dense heterogeneities along the central latitude of 58°S.***

SST – South Sandwich Trench

VIII.1 *Distribution of dense heterogeneities along the central latitude of 58°S between depths of 1-100 km*

The Scotia Sea region is considered along several latitudinal and longitudinal cross-sections (Figure a). Background map is the bottom topography. The vertical cross-section of the harmonical dense anomalies along 58°S latitude is shown in the Figure b.

It is seen that the Scotia's body is extended up to depths of 100 km. The roots of the SS Island ridge (1) are sloped to the Scotia Sea side and are immersed into depths 25-30 km along distance 500 km. Masses of the South Sandwich Trench (2) is indicated up to depth of 20 km.

A joint area of the Shackleton FZ and the Western Scotia Ridge is marked as the (3) zone.

Thickness of the crust within the central part of the Scotia Sea is 4 km between 30°-40°W and is increased up to 6-8 km between 40°-50°W.

VIII.2 ***Section along the 58°S between depths of 390-2800 km***

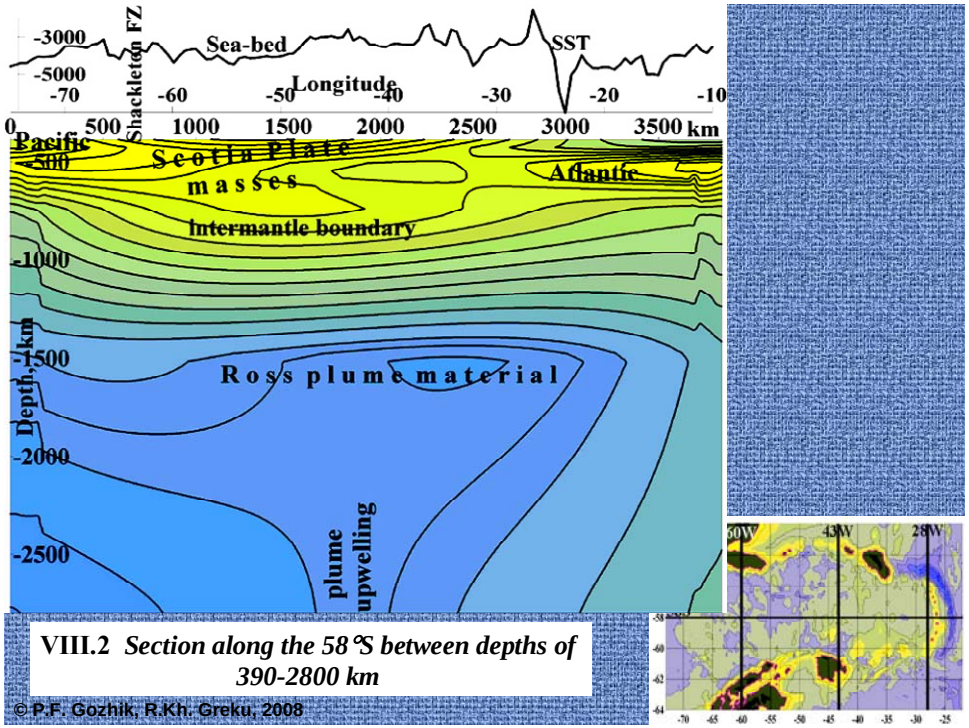

VIII.2 ***Section along the 58°S between depths of 390-2800 km***

VIII.2 ***Section along the 58°S between depths of 390-2800 km***

Extension of the Ross plume material is observed beneath the Scotia Sea at the cross-section along the central latitude of 58°S. Two mantle flows coming from the west (lateral) and from the area below the Weddell Sea (ascending) are shown. The transition layer's thickness is between depths from 620-850 km up to 1400 km. The plume material is extended from the west at the depth of 1500 km up to 20°W-15°W. It confirms the prediction of a possible generating of the mantle flow from the Pacific through the Drake Passage [19]. Figure shows the sheet of the Pacific mantle masses from the west and the Atlantic mantle masses from the east into a narrow layer of 500-610 km. The Scotia Microplate is up to 310 km thick and it is moved by the Atlantic masses significantly westward beginning from the depth of 200 km.

VIII.3 ***Section along the meridian of 60 °W***
SShT – South Shetland Trench

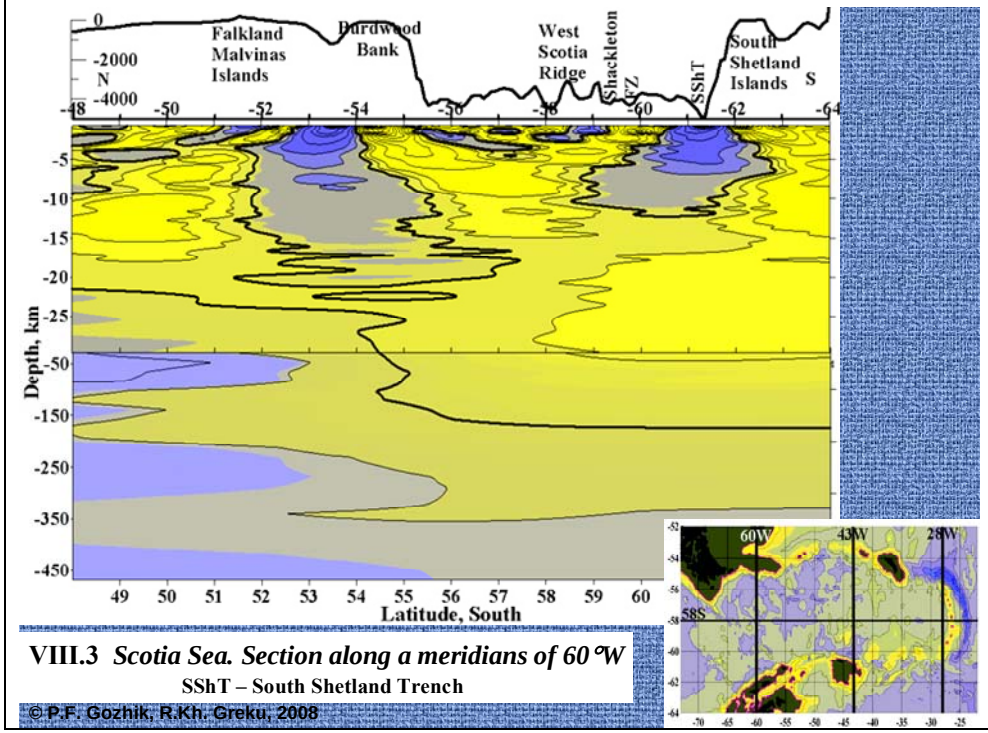

VIII.3 ***Scotia Sea. Section along a meridians of 60 °W***
SShT – South Shetland Trench

40_section_Scotia43w_RGB_SMYK.tif, 40_map_RGB_SMYK.tif
VIII.4 ***Section along the meridian of 43 °W***

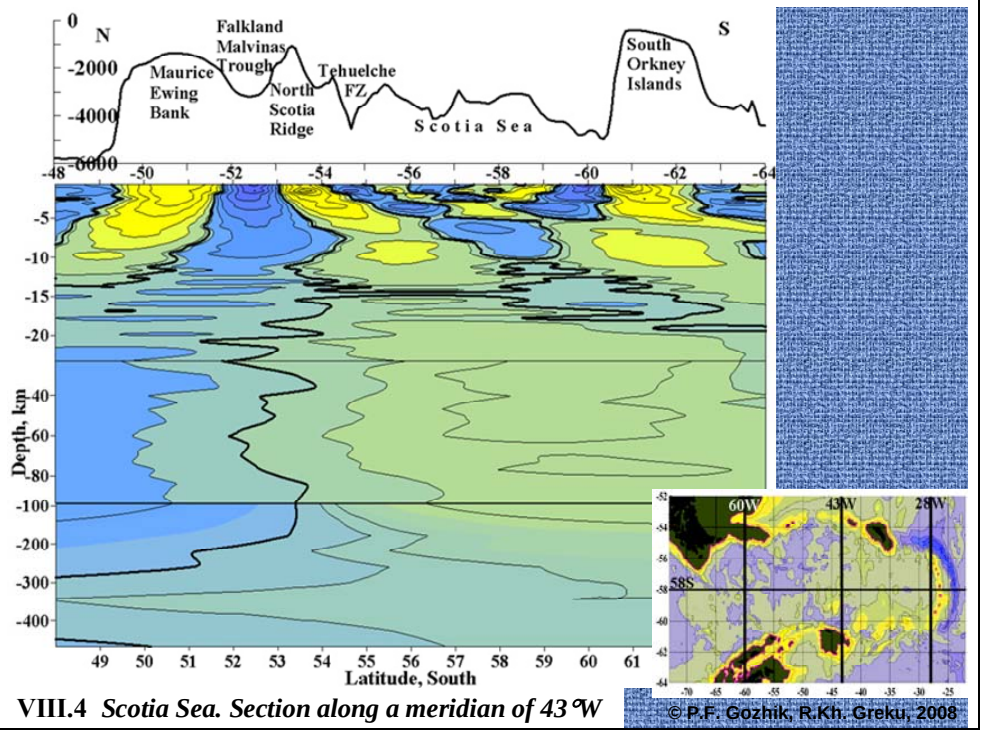

VIII.4 ***Scotia Sea. Section along a meridian of 43 °W***

VIII.5 *Section along the meridian of 28 °W*

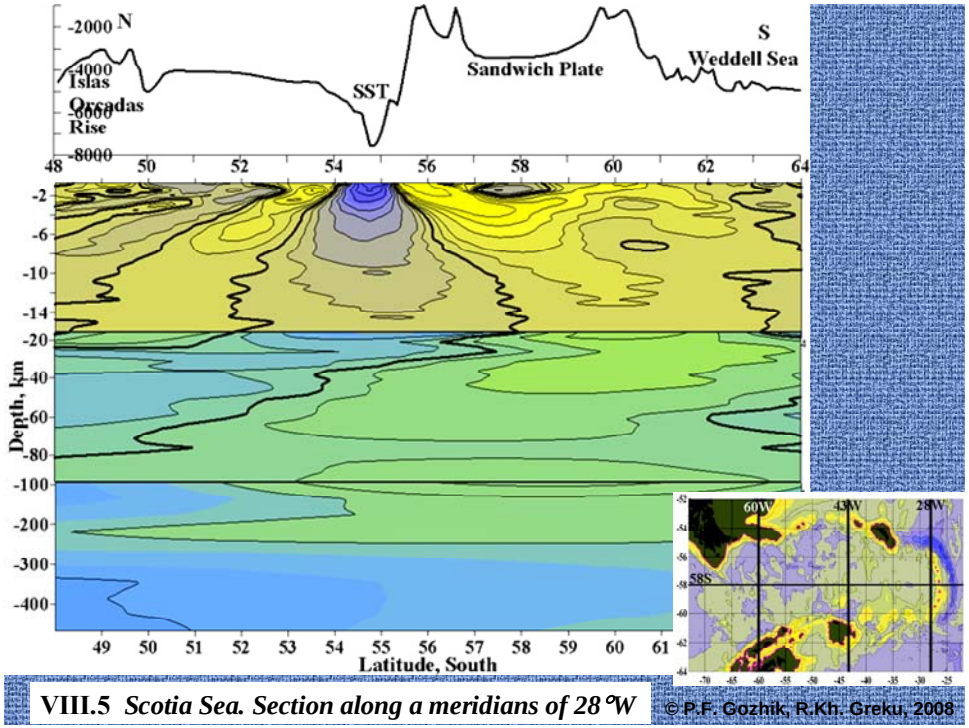

VIII.5 *Scotia Sea. Section along a meridians of 28 °W*

REFERENCES

1. 1 Bijwaard H., Spakman W., Engdahl E. R. Closing the gap between regional and global travel time tomography, J. Geophys. Res., 1998, 103, B12, 30,055-30,078.
2. Greku R.Kh., Usenko V.P., Greku T.R. (2006) Geodynamic Features and Density Structure of the Earth's Interior of the Antarctic and Surrounded Regions with the Gravimetric Tomography Method. In:. Fütterer D.K., Damaske D., Kleinshmidt G., Miller H., Tessensohn F. (eds) Antarctica - Contributions to global earth sciences. Springer, Berlin Heidelberg New York, pp. 369-375.
3. Moritz H. 1990. The Figure of the Earth. Theoretical Geodesy and the Earth's Interior. Wichmann, Karlsruhe.
4. Brown R.D., Khan W.D., McAdoo D.C. et al., 1983. Roughness of the Marine Geoid from altimetry. J. Geophys. Res., 88, C3, 1531-1540.
5. Gahagan L.M., Scotese C.R., Royer J-Y., et al., 1988. Tectonic fabric map of the ocean basin from satellite altimeter data. Tectonophysics, 155, 1-26.
6. Gainanov A.G. Geology and Geophysics of the Eastern Indian Ocean Floor (by the 54 and 58 cruises data of the RV Vityaz). – Moscow, Nauka, 1981. –256 p. (in Russian)
7. Allan R.R. Depth of sources of gravity anomalies. “Nature. Phys. Sci.”, 1975, 236, #63, 22-23.
8. Greku R.Kh., Greku D. R. Interaction of Antarctica with other regions at different spatial scales and deep layers. Cooper, A.K., P.J. Barrett, H. Stagg, B. Storey, E. Stamp, W. Wise, and the 10th ISAES editorial team, eds. (2008). Antarctica: A Keystone in a Changing World. Proceeding of the 10th International Symposium on Antarctic Earth Sciences. Washngton, DC: The National Academics Press. Online Proceedings (http://pubs.usgs.gov/of/2007/1047/).
9. Greku R.Kh.,. Greku T.R. Deep structure of the Antarctic Plate’s boundary zone by the gravimetric tomography method. Cooper, A.K., P.J. Barrett, H. Stagg, B. Storey, E. Stamp, W. Wise, and the 10th ISAES editorial team, eds. (2008). Antarctica: A Keystone in a Changing World. Proceeding of the 10th International Symposium on Antarctic Earth Sciences. Washngton, DC: The National Academics Press. Online Proceedings (http://pubs.usgs.gov/of/2007/1047/).
10. Greku, R. Kh, T. R. Greku (2006), Mantle and crustal structure of Antarctic along 170°W and 44°E meridians with the gravimetric tomography technique,

in: Terra Antarctica Reports, No. 12, Proceedings of the Workshop on Frontiers and Opportunities in Antarctic Geosciences 2004, edited by C. Siddoway and C. A. Ricci, pp 145-154, Terra Antarctica Publication, Siena, Italy.

11. Shimbirev B,P., Theory of the Earth's Figure, Moscow, Nedra, p. 431, 1975 (in Russian).
12. Dziewonski A.M., Anderson D.L., 1981. Preliminary Reference Earth Model. Phys. Earth Planet. Inter., 25, 297-356.
13. H. Rapp, Y. M. Wang, and N. K. Pavlis, The Ohio State 1991 Geoptential and Sea Surface Harmonic Coefficient Models, 410, Dept. of Geodetic Sci. and Surv., Ohio State Univ., 1991.
14. Lythe, M., Vaughan, D., and the BEDMAP Consortium (2001): "BEDMAP: A new ice thickness and subglacial topographic model of Antarctica". Journal of Geophysical Research, 106(B6): 11335-11351.
15. Murphy J.B., Oppliger G.L., Brimhall G.H. Plume-modified orogeny: and example from the western United States// Geology, 1998, V. 26, P. 731-734.
16. Ishii M. and J.Tromp (2004), Constraining large-scale mantle heterogeneity using mantle and inner-core sensitive normal modes, Physics of the Earth and Planetary Interiors, 146, 113–124.
17. Voronov P.S., 1964. Tectonic and neotectonic of Antarctica. In: *Antarctic geology, SCAR Proceeding*, Amsterdam.
18. Bird, P. (2003), An updated digital model of plate boundaries, An Electronic J. of the Earth Sci., Volume 4, Number 3, 14 March 2003, doi:10.1029/2001GC000252.
19. Andersen, O. B., P. Knudsen and R. Trimmer, Improved high resolution gravity field mapping (the KMS02 Global Marine gravity field). In press, IAG symposium, 126, Sapporo, 2004.
20. Lonsdale, P. (1994), Geomorphology and structural segmentation of the crest of the southern (Pacific-Antarctic) East Pacific Rise, J. Geophys. Res., 99, B3, 4683-4702.
21. Storey, B.C. (1995), The role of mantle plumes in continental breakup: case histories from Gondwanaland, Nature, 377, 28, 301-308.
22. Ritzwoller, M. H., N. M. Shapiro, A. L. Levshin and G. M. Leahy (2001), Crustal and upper mantle structure beneath Antarctica and surrounding

oceans, J. Geophys. Res., 106, 12, 30645-30670.

23. Galindo-Zaldívar, L., L. Gamboa, A. Maldonado, S. Nakao et al. (2006), Bransfield Basin tectonic evoluton, in: Antarctica - Contributions to Global Earth Sciences, Proceedings of the IX International Symposium of Antarctic Earth Sciences Potsdam, 2003, edited by D. K. Fütterer, D. Damaske, G. Kleinshmidt, H. Miller and F. Tessensohn, pp.243-248, Springer, Berlin Heidelberg New York.

24. Schöne, T. (1997), The gravity field in the Weddell Sea, Antarctica, by radar altimetry from Geosat and ERS-1, Berichte zur Polarforschung, 220, Alfred Wegner-Inst fur Polar- und Meer-esforchung, Bremerhaven, Germany, pp. 145.

25. Canals, M., E. Gràcia, M. J. Prieto and L.M. Parson (1997), The very early stages of seafloor spreading: the Central Bransfield Basin, NW Antarctic Peninsula, The Antarctic Region: Geological Evolution and Processes, 669-673.

26. Leat Ph. (2002), Tracing mantle flow beneath the Scotia Sea, www.antarctica.ac.uk, British Antarctic Survey.

27. Turcotte, D. L. & Schubert, G. 2002. Geodynamics, 2nd ed. Pp. 456.